

**MODELLING OF ELECTROMAGNETIC
DEBRIS IN SPACE BY AN EVACUATOR**

BY

**ODIMAYOMI, PETER KAYODE
(M. ENG./SEET/2007/1871)**

**DEPARTMENT OF ELECTRICAL AND COMPUTER
ENGINEERING, FEDERAL UNIVERSITY OF
TECHNOLOGY, MINNA, NIGER STATE**

DECEMBER, 2010

MODELLING OF ELECTROMAGNETIC DEBRIS IN SPACE BY AN EVACUATOR

BY

ODIMAYOMI, PETER KAYODE

(M. ENG./SEET/2007/1871)

A THESIS SUBMITTED TO THE POSTGRADUATE SCHOOL IN
PARTIAL FULFILLMENT OF THE REQUIREMENTS FOR THE
AWARD OF M. ENG. DEGREE IN COMMUNICATION
ENGINEERING, DEPARTMENT OF ELECTRICAL AND
COMPUTER ENGINEERING, FEDERAL UNIVERSITY OF
TECHNOLOGY, MINNA, NIGER STATE.

DECEMBER, 2010

DECLARATION

I declare that this thesis "*Modelling of Electromagnetic Debris in Space by an Evacuator*" was done by me and has never been presented elsewhere for the award of a Master Degree. It is the result of my own research work except for works cited in the references.



Odimayomi, Peter Kayode

09/02/2011

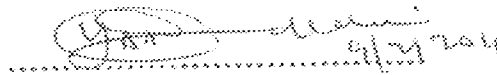
Date

CERTIFICATION

The thesis titled "*Modelling of Electromagnetic Debris in Space by an Evacuator*" by Odimeyomi Peter Kayode (M.Eng/SEET/2007/1871) meets the regulation governing the award of the degree of Master of Engineering (M.Eng) of the Federal University of Technology, Minna and is approved for its contribution to scientific and literary presentation.

Engr. (Dr.) Y.A. Adediran

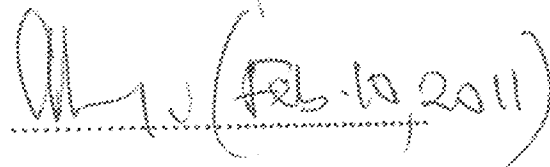
Supervisor


..... 2/2/2011

Signature and Date

Engr. A. G. Raji

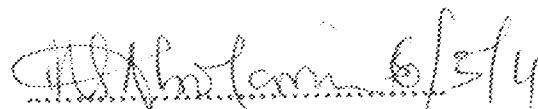
Name of Head of Department


..... (Feb. 10, 2011)

Signature and Date

Prof. M.S. Abolarin

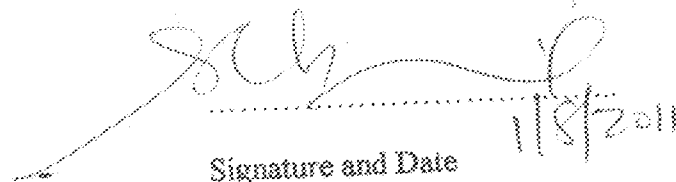
Dean, SEET


..... 6/5/11

Signature and Date

Prof. (Mrs) S. N. Zubairu

Dean, Postgraduate School


..... 1/8/2011

Signature and Date

ACKNOWLEDGEMENTS

It is a great thing to have a vision but the mission of accomplishment turns great dreams into reality. Foremost, I acknowledge the leading of the Holy Spirit, who planned this programme and granted me grace throughout the period.

My gratitude goes to Dr. Y.A. Adediran, my project supervisor, it is believed that no individual is ever made without event and history. My encounter with him gave me opportunity to appreciate dedication, loyalty and fear of God. Far more than anything, his responsiveness to duty has built a new life in me.

I want to also appreciate the Head of Department, the departmental Postgraduate coordinator, the Dean School of Engineering and Engineering Technology and the Dean of Postgraduate School and the entire members of staff for their immersed assistance throughout my programme.

I also appreciate the support of my wife, Mrs. Taiwo Olaide Odimayomi for her understanding during the period of the programme.

I also appreciate the Management of National Space Research and Development Agency (NASRDA) who initiated and provided financial support for the Master Degree programme. To my colleagues, their team spirit was inspirational throughout the programme.

ABSTRACT

The global communication, navigation and remote observation of the Earth and other galaxies have tremendously enjoyed the use of satellite technology and applications. These satellites at the end of life are de-orbited and ejected into the graveyard orbit where they litter the space environment. Collisions during the operation of these satellites and at their end of life cause breakups, thus producing space debris which are dangerous to other operational satellites and the launch of a new one. Most recent efforts to mitigate space debris have been in the formulation of rules and regulations for design and launching of satellites to avoid creation of space debris. The Electromagnetic Space Debris Evacuator developed is a model simulated using MATLAB software. The thesis demonstrated that small sizes of space debris in the range of 10 μm to 10 cm diameter or average mass of 15 to 150 milligrams can be evacuated by "Electromagnetic Space Debris Evacuator" from the space orbits, thus reducing the dangers their collision with operational satellites might cause. The result of this work would add to the current efforts of the United Nations' effort in mitigation of space debris. The simulated result compares favourably with the ideal magnetic curve, which shows that the simulated value conforms to the modelled equation with respect to the parameters (Magnetomotive force, Flux density, Cross-sectional area and length of coil) of the model can be varied to achieve desired magnitude of electromagnetic flux for evacuation of space debris in orbits.

TABLE OF CONTENTS

	Page
Declaration	ii
Certification	iii
Acknowledgements	iv
Abstract	v
Table of Contents	vi
List of Tables	ix
List of Figures	x
List of Plates	xii
Abbreviations and Symbols	xiii
CHAPTER ONE	
1.0 INTRODUCTION	1
1.1 Satellite Systems and Space Debris	1
1.1.1 Space Segment	2
1.1.2 Ground Segment	6
1.1.3 Satellite Orbits	7
1.2 Space Debris	9
1.2.1 Evolution of Space Debris	10
1.2.2 Observation of Space Debris	11
1.3 Effects of Debris on Space Environment	15

1.3.1	Effects of Large Debris	15
1.3.2	Effects of Small Debris	16
1.3.3	Debris Collision Impact	17
1.4	Statement of the Problem	17
1.5	Aims and Objectives	18
1.6	Methodology	18

CHAPTER TWO

2.0	LITERATURE REVIEW	20
2.1	Examples of damages caused by space debris	24
2.2	United Nations Intervention Programme for Space Debris Mitigation	25
2.3	Review of Past Efforts	26
2.3.1	Natural Mechanism	27
2.3.2	Laser Model	28
2.3.3	Electro-dynamic Tether for Active Debris Removal	29
2.3.4	Generic Inflatable De-Orbit device for Satellite	31
2.3.5	Space Shuttle Evacuator	37
2.3.6	The Proposed Electromagnetic Space Debris Evacuator	37

CHAPTER THREE

3.0	MATERIALS AND METHODS	39
3.1	Features and Integration of Electromagnetic Evacuator Model	41
3.2	Mathematical Modelling of the Space Debris Evacuator Parameters	44
3.2.1	Magnetomotive force in the Space Debris Evacuator	44

3.2.2	Electromagnetic Flux in the Space Debris Evacuator	45
3.2.3	Parameters of Panel A	47
3.3	In-Orbit Positioning of Debris Evacuator	51
3.4	Atmospheric Entry of Debris Evacuator	52
CHAPTER FOUR		
4.0	RESULTS	54
4.1	Analysis of the plot of magnetomotive force (F) against electromagnetic flux (q) in each panel in the Debris Evacuator	55
4.2	Analysis of the plot of Length of coil (l) against Magnetomotive Force (F) in the Debris Evacuator	57
4.3	Analysis of the plot of magnetomotive force (F) against Total electromagnetic flux (Q_{total}) for the Debris Evacuator	59
CHAPTER FIVE		
5.0	DISCUSSION, CONCLUSION AND RECOMMENDATIONS	62
5.1	Discussion	62
5.2	Conclusion	63
5.3	Recommendations	63
REFERENCES		65
APPENDICES		68

LIST OF TABLES

Table	Page
1.1 LEO space debris source size ranges	13
2.1 Values for drag area and ballistic coefficient	33
4.1 MATLAB values for the simulation of magnetomotive force (F) against electromagnetic flux (q) in each panel in a unity cross-sectional area (A) and relative permeability environment (μ_r) of the debris evacuator	56
4.2 MATLAB values for the simulation of length of coil (l) against Magnetomotive Force (F) in each panel in a unity cross-sectional area (A) and relative permeability environment (μ_r) of the debris evacuator.	58
4.3 MATLAB values for the simulation of magnetomotive force (F) against Total electromagnetic Flux (Q_{total}) of the debris evacuator in a unity cross-sectional area (A) and relative permeability environment (μ_r) of the debris evacuator.	61

LIST OF FIGURES

Figure	Page
1.1 Satellite Fairing	4
1.2 Satellite Perturbation Graph	5
1.3 Space Debris Generation	14
1.4 Plot of Debris Flux versus Diameter as Determined by Multiple Instruments and Studies	15
2.1 Classes of Space Objects	22
2.2 Number of Satellites and their Orbits	23
2.3 iDod Design Process	32
2.4 STK de-orbit Prediction	34
3.1 Block Diagram of Space Debris Evacuator	39
3.2 Illustration of Debris Evacuator and Attracted Space Debris in Orbit	41
3.3 Configuration of the Developed Electromagnetic Debris Evacuator	42
3.4 In-orbit Configuration of the Developed Model of Debris Evacuator	43
3.5 Objects in Near-earth Space and their Respective Contribution to Space Debris Environment, Including Meteoroids	50
4.1 Plot of Magnetomotive Force against Panel Electromagnetic Flux	55
4.2 Plot of Length of Coil against Magnetomotive Force	57
4.3 Plot of Magnetomotive Force against Total Electromagnetic Flux	60

LIST OF PLATES

Plate	Page
I. Satellite Integration	4
II. Satellite Maneuvering in Orbits	8
III. The Orbital Position of GEO Satellite in Orbits	12
IV. Dead Satellites as Debris in Orbits	12
V. iDod Pyramid Concept	35
VI. iDod Storage Device	35

ABBREVIATIONS

AIAA	American Institute of Aeronautics and Astronautics
AIT	Assembly Integration and Testing
AOCS	Attitude and Orbit Control System
BBE	Base-Band Equipment
BNSC	British National Space Centre
CNES	Centre National d'Etudes Spatiales
CNSA	China National Space Administration
COPUOS	Committee on the Peaceful Uses of Outer Space
DLR	Deutsches Zentrum für Luft- und Raumfahrt e.V
EOL	End of Life
EPS	Electrical Power Subsystem
ESA	European Space Agency
ERS-1	European Remote Sensing satellite
EMS	Electro-magnetic Control Subsystem
CGG	Cool Gas Generator
GEO	Geosynchronous Earth orbit
GTO	Geostationary Transfer Orbit
HEO	High Earth orbit
ISRO	Indian Space Research Organisation
IAA	International Academy of Astronautics
IADC	Inter-Agency Space Debris Coordination Committee

ISA	Italian Space Agency
ISS	International Space Station
JAXA	Japan Aerospace Exploration Agency
LDEF	Long Duration Exposure Facility
LEO	Low Earth Orbit
LEOP	Launch Early Orbit Phase
MEO	Medium Earth Orbit
MLI	Multilayer Insulation
NSAU	National Space Agency of the Ukraine
NASRDA	National Space Research and Development Agency (of Nigeria)
NASA	National Aeronautics and Space Administration
NOC	Network Operating Centre
PCB	Programmable Circuit Board
RF	Radio Frequency
ROSCOSMOS	Russian Federal Space Agency
SCC	Satellite Control Centre
SEDS-2	Small Expendable Deployer System-2
SPOT-2	Satellite Pour l'observation de la Terre
SSN	Space Surveillance Network (USA)
SSS	Space Surveillance System (Russia)
TTC&M	Telemetry, Tracking, Command and Monitoring
TT&C	Telemetry, Tracking and Control
TC&R	Telemetry, Command & Ranging

TC/TM	Telecommand/Telemetry Signal
UHF	Ultra High Frequency
UPS	Unified Propulsion Subsystem
USSN	United States Space Surveillance Network
UN	United Nations
VHF	Very High Frequency

SYMBOLS

$C_D A$	drag coefficient x reference area (m^2)
C_L	aerodynamic lift coefficient
G_c	gravitational constant = $1(kg.m/N.s^2)$
g	acceleration due to gravity (m/sec^2)
q	flux in each panel of evacuator (Weber)
Φ	total flux in the evacuator (Weber)
R	planet radius (m)
r	altitude plus planet radius (m)
t	time (sec)
V	velocity (m/sec)
V_∞	escape velocity (m/sec)
W	mass of debris (kg)
μ	permeability
γ	flight path angle measured positive down from local horizontal (deg)
ρ	free stream density (kg/m^3)

CHAPTER ONE

1.0

INTRODUCTION

1.1 Satellite Systems and Space Debris

Satellite is a man-made object in the sky (orbit) that rotates around the Earth in a given period of time depending on the height (altitude) from the Earth surface. The satellite system comprises the communication payload and the platform depending on the satellite services: communication, remote sensing, navigation, reconnaissance, surveillance and meteorological services. When these satellites get to their end of life or have a collision with other satellites in the orbit they generate the space debris. The buildup of these debris create threats to functional satellites in the orbits, hence the phenomenon must be addressed.

The life span of a satellite in orbit depends on source of power supply for its onboard electronics and the amount of fuel carried in the satellite. The satellite systems consist of space segment and ground segment. The space segment comprises the platform (also called the bus) and the mission module. The space segment is the actual component of the system called "Satellite" which is launched into space orbit for the required services. In this proposed work, the mission module is an electro-magnetic panel.

The ground segment, comprising the baseband equipment and antenna, is located in preferred and carefully selected areas free from any environmental interference. It controls the space segment throughout useful or operational life and is also used for de-orbiting the satellite to the disposal (graveyard or parking) orbit.

1.1.1 Space Segment

The satellite space segment is a combination of subsystems which are responsible for management of the satellite services and the control of the satellite. They are:

- i. Antenna system
 - ii. Attitude and Orbit Control System (AOCS)
 - iii. Telemetry, Tracking, Command and Monitoring (TTC&M)
 - iv. Structure and Thermal system
 - v. Power and system and Communication payload
- The Antenna system is the appendages that are deployed immediately the satellite fairing is opened to commence communication with the ground segment for major control and maneuvering of the satellite to its operational orbit and subsequent normal operation till end of life.
 - The AOCS is responsible for the control and stabilization of the satellite in the operational orbit by accepting telecommand from the TT&C subsystems onboard; and, with respect to the degree of the drift, it automatically maneuvers the satellite back to original and expected position. Thereafter, it will send telemetry to the ground segment about the current position of the satellite.
 - The TTC&M is the subsystem that receives telecommand from the ground segment and directs it to appropriate subsystem for immediate reaction with respect to the health check and alert. It is also responsible for continuous sending of telemetry to the ground segment counterpart TTC&M for preparation of corrective telecommand.

- The power system is responsible for generation and distribution of electricity to all parts of the satellite system. The entire power onboard is generated from the solar panel arrays and bank of batteries, which supply power directly to the satellite system during the day and part of the solar energy is used for charging the batteries to power the system at night and during ellipse. The power system determines the end of life of a satellite.
- The Communication payload is the main module that offers the services of the satellite mission. This subsystem contains the amplifier system which boosts the weak signal coming from the Earth and carry out the frequency conversion. In other words, the communication payload carries the module that does the main service of the satellite launch (mission definition).

The integration of these space segment subsystems are carefully interfaced together and coupled into platform system (structure and thermal subsystems) for subjection to different examinations and testing such as antennas and solar arrays test, alignment and leak test. Other tests are thermal and vacuum test, system sine vibration, shock and acoustic test. These tests are carried out to ensure radiation pattern of spacecraft in the ground and space environment of operation. The integrated satellite, after due testing, is adapted to the launcher (rocket) at the Assembly Integration and Testing (AIT) centre where launch readiness and simulation are carried out. Thereafter, the final integrated system is taken to the launch pad for delivery of satellite into the pre-determined orbit.

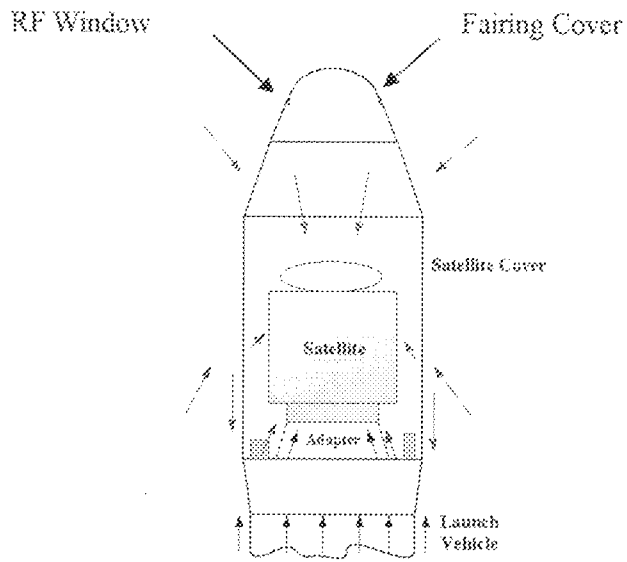


Fig. 1.1: Satellite Fairing [Timothy *et al*, 2003].

The well-interfaced satellite is placed in a fairy; and, with the aid of an adapter, it is coupled to the launcher (rocket) as shown in Fig. 1.1 and Plate I for flight to the desired orbit.

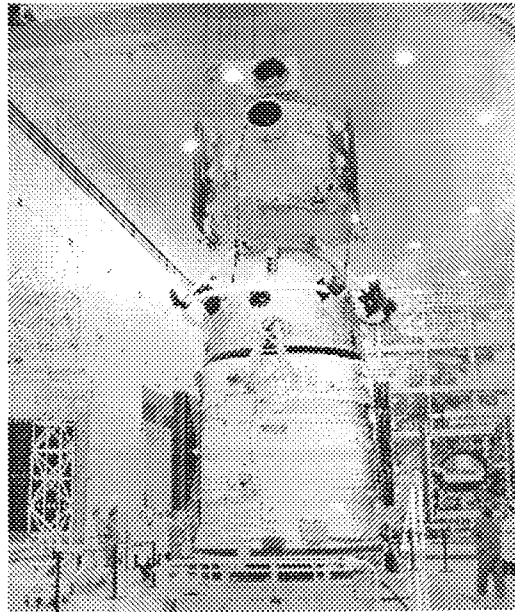


Plate I: Satellite Integration [Timothy *et al*, 2003]

In the process of launch, several parameters are considered. These include:

- Earth's oblateness: the earth bulges at the equator, which leads to a much more complex gravity field than the spherically symmetric field of a 'point' gravity source.
- Solar and lunar effects: these effects of the sun and moon, respectively, are the most influential gravitational forces on earth satellites besides the earth's own field.
- Atmospheric drag: the friction that a satellite encounters as it passes through the diffuse upper layers of the earth's atmosphere.
- Solar radiation pressure: solar radiation pressure is caused by collisions between the satellite and photons radiating from the sun, which are absorbed or reflected.

The combination of these perturbations on the launched satellite is shown in fig. 1.2. These forces tend to affect the acceleration of the satellite with respect to the distance (altitude) covered in the direction of the planned trajectory to the desired orbit.

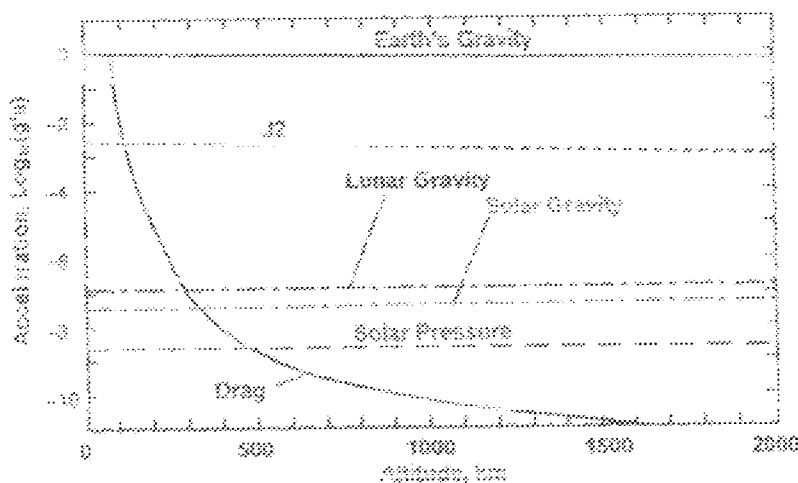


Fig. 1.2: Satellite perturbation graph [Iberesa, 2004]

1.1.2 Ground Segment

The ground segment is the second component of the satellite systems comprising the antenna and base-band equipment, which are installed in a preferred location and is mostly called Ground Control Station. The basic responsibilities of the ground segment are control of the space segment (satellite) and monitoring of the deployed services, in the case of communication satellite.

The ground segment can be divided into two groups, based on the above-stated responsibilities, as:

- i. Telemetry, Tracking and Control (TT&C)
- ii. Network Operation Centre (NOC)

The TT&C also houses a section called Satellite Control Centre (SCC), which is responsible for the comparison of received telemetry data from the TT&C Base-Band Equipment (BBE), and make necessary orbit calculations with respect to the degree of drift. It will also derive the amount of fuel required for the maneuvering. These control parameters are written in scripts and sent to the satellite through the TT&C section as "telecommand", for the orbit (drift) correction. The SCC is crucial to the ground segment and the main functions are:

- i. Processing of real-time telemetry and tracking data
- ii. Generation and transmission of satellite command instructions.
- iii. Satellite orbit determination, ephemeris prediction, Orbit control parameters and strategy
- iv. Controlling the precision calibration and Satellite status monitoring

- v. Archiving of system and telecommands information and System status monitoring
- vi. Display and recording of calculation results

The Network Operating Centre (NOC) monitors the carrier frequency, power and other transmission parameters of the services deployed by the satellite. That is, the control centre is used for monitoring the subscriber's operation in compliance with the requirements as signed in the agreements. The ground segment is responsible for the health check of the satellite until end of life and final de-orbiting to the graveyard orbit.

1.1.3 Satellite Orbits

Satellite orbits are in the region ranging from 200 km above the Earth and are categorized according to this distance as follows:

- The distance of 200 km to 800 km is called Low Earth Orbit (LEO), used for the launch of earth observation and remote sensing satellites.
- The distance of 800 km to 2,000 km is called the Medium Earth Orbit (MEO), used for launch of communication satellites like Iridium and navigation satellite – Galileo and GLONAS in constellations
- The region of 36,000 km is called the Geostationary Earth Orbit (GEO), used for the launch of communication satellite

Concerted efforts are required to place satellites into these orbits because of the Earth gravitational pull. Rockets are used with thrust in opposite direction of the Earth force to deliver the satellites to the pre-determined orbits. As a result of the perturbation experience on the satellite in the orbit, different stabilization mechanisms are designed in

the satellite such as: Spin stabilization, Dual-Spin stabilization, Gravity-Gradient stabilization and Three-Axis stabilization. An operational satellite is perpetually maintained in the operational orbit (through station keeping) through the North/South (N/S) maneuver for inclination correction and East/West (E/W) maneuver for semi major axis and eccentricity correction. The orbital tolerant drift, called dead band, must not be more than 0.5 degree in both E/W and N/S orientation. The launch maneuvering of satellite into the orbit is shown in Plate II, which illustrates the flight of the satellite to the orbit.

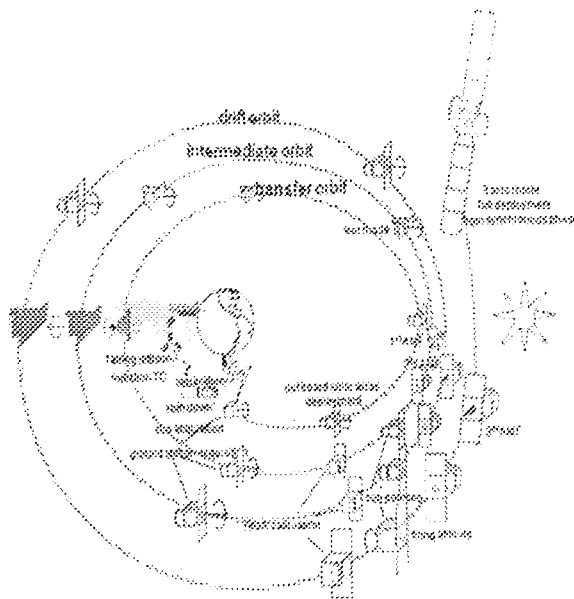


Plate II: Satellite maneuvering in orbits [Timothy *et al*, 2003]

In the process of the satellite launch, different orbits are used (as seen in Plate II) to achieve in-orbit of the satellite such as:

- Parking Orbit, a temporary orbit which provides a safe and convenient location for satellite checkout and storage between operations.
- Transfer Orbit, used for getting from place to place. Examples are the transfer orbit to geosynchronous altitude and interplanetary orbit to Mars [Timothy *et al*, 2003].

The duration (end of life or lifespan) of the satellite in orbit is constantly subjected to perturbation and subsequent maneuvering (station keeping) and depends on the amount of fuel carried by the satellite, lifespan of the satellite battery and the charging system of the solar panels. After exhausting the pre-planned percentage of total fuel in the satellite meant for station keeping till end of life (i.e. lifespan of satellite), the satellite is de-orbited from that orbital slot. This is done to avoid collision with another spacecraft since the ground station can no longer manage the re-positioning of the satellite (station keeping). Rather than allow it to continue to dangle in the useful orbit, the pre-designed amount of fuel reserved for transfer of the satellite to disposal orbit is used to maneuver the satellite from the operational orbit to kilometres further away from its original position. The region where such satellites are kept is called disposal orbit, graveyard orbit or parking orbit.

In the case of Nigerian Communication Satellite (NigComSat-1) for example, the disposal orbit is 140 km away from its initial operational orbit. This is similar for most geostationary satellites.

1.2 Space Debris

For over 50 years, from the launch of Spumik on 4th October 1957 up to 1st January 2008, approximately 4,600 launches have placed some 6,000 satellites into orbit, out of which about 400 are missions beyond geostationary orbit or on interplanetary trajectories [Megan, 2009]. At the early satellite launch, when a satellite reached its end of life, operators simply abandoned the spacecraft in the orbit without control. These, plus spent booster stages and other fall-off parts, stayed up in the orbit until the decay of such orbit with the satellites falling back to Earth, or colliding with each other. Also, batteries,

pressurized systems, and fuel tanks could explode, adding to the debris population. These generated debris, which contribute to the growing particle population, ranging from less than a micrometer to 10 centimetres or more in size. In orbit, relative velocities can be quite large, ranging in the tens of thousands of kilometre per hour.

1.2.1 Evolution of Space Debris

Today, it is estimated that only 800 satellites are operational - roughly 45 percent of these are both in LEO and GEO. Space debris comprise the ever-increasing amount of inactive space hardware in orbit around the Earth as well as fragments of spacecraft that have broken up, exploded or otherwise become abandoned. These occurrences are responsible for about 9,000 space debris currently being observed [Megan, 2009]. These debris are measured both from ground-based and space-based equipment and are categorized according to sizes and masses. The break-up of satellites and other fall-off from satellite, such as leaked fuel, paint flakes and thermal blankets create the fragmented space debris. This category forms about 42% of the space debris, while rocket bodies and boosters are about 17%. The manned mission deployments generate about 19% and the non-functional spacecrafts constitute about 22% of 100% of debris in the space environment [Christiansen et al, 1996].

The need for protection of satellite against space debris has caused an increase in the cost of satellite design and launch. Some recorded cases such as tiny rocks, paint flecks and other fragments of junk whizzing around the Earth, posed the greatest threat to the shuttles and the astronauts on board, according to the preliminary results of a new NASA risk study [Johnson et al, 2004]. Findings have shown that the foreign object hitting the shuttle as it flies through space causes catastrophic damage [United Nations, 1999]. Until now,

some researchers assumed space debris to be on the same level as the danger seen during the shuttle's treacherous launch or its fiery plunge back through the atmosphere to land. The internal risk assessment, still under review by the space experts, states that space debris hitting different parts of the spacecrafts in orbit account for 11 of the 20 problems most likely to cause the loss of another shuttle and crew. Studies have also shown that space debris accounts for half of the catastrophic risk on any flight [United Nations, 1999]

1.2.2 Observation of Space Debris

There are two major ways of observing the space debris. These are:

- i. Ground-based observation using Radar and Optical instruments
- ii. Space-based observation using Retrieved surfaces and impact detectors

Typically, radar observations have been used for space debris in Low Earth Orbit (LEO), while optical observations have been used for High Earth Orbit (HEO).

For passive optical observation, the signal intensity return is inversely proportional to the square of the distance or altitude of the object since the incident illumination from the Sun is essentially independent of altitude. The space environment which surrounds the Earth is becoming increasingly polluted with debris. Currently, the United States Space Surveillance Network (USSN) is using ground-based radar, optical and infrared sensors to track more than 7,500 objects. The minimum size of a trackable object is about 10 cm for a low Earth orbit, and about 1 m for the geostationary orbit. Only about 6% of these catalogued objects are active satellites. Over 40% are fragments of disintegrated satellites and upper stages of rockets [Christiansen *et al.*, 1996]. The placement of satellites in the

operational orbits and subsequent positions as debris after end of life is shown in Plate III and Plate IV respectively.

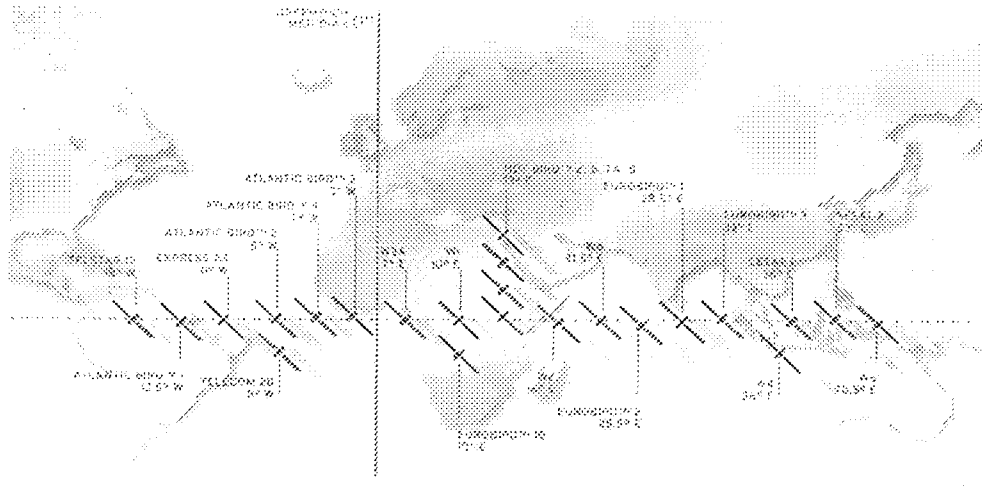


Plate III: The orbital position of GEO satellite in orbits [United Nations, 1999].

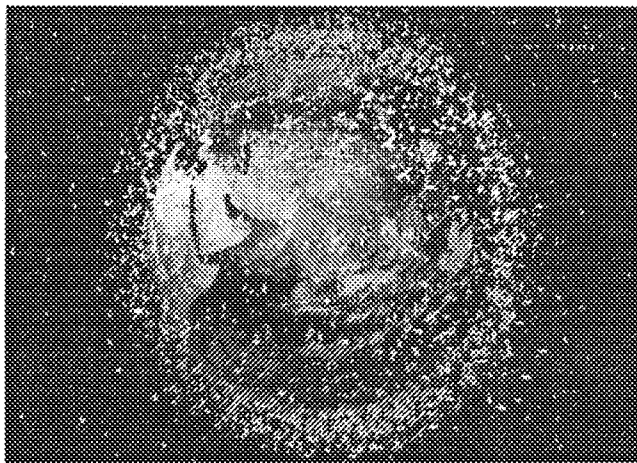


Plate IV: Dead Satellites as debris in orbits [Johnson *et al*, 2004].

Several efforts and methodologies have been presented which categorize and catalogue the orbital debris. Others considered the order of size and time of debris creation. The first collision and risk assessment carried out by NASA was on the International Space Station and Space Shuttle. Other space assessment is the un-catalogued fragments from recent

breakups. It is estimated that the numbers of objects larger than 1 cm range from 30,000 to 100,000 pieces orbiting the Earth. Other observations of debris are categorized in size ranges as shown in Table 1.1.

Table 1.1. LEO Space debris source size ranges in-orbit as at 2006 [Stansbery *et al.*, 2005].

S/N	Orbital debris source	Size range	How observed	Primary instrument	Estimated number
1	Payloads and rocket bodies past end-of-life	>5 cm	Tracked and cataloged	SSN radars	3,600
2	Mission-related	<1m	Tracked and cataloged	SSN radars	1,270
3	Fragments of in-orbit	<1m	Tracked and cataloged	SSN radars and Haystack	Unknown
		<10cm	observed statistically	HAX radars	>1,000,000
4	Sodium potassium coolant droplets	~1-5m	Observed statistically	Haystack and HAX radars	~55,000
5	Solid rocket motor char, slag, and dust	~1-5m	Observed statistically	Returned surfaces, ground-based tests	Unknown
6	Ejecta and paint flakes (degradation products)	<1mm	Observed statistically	Returned surfaces	Unknown
7	Meteoroids	<1 cm	Observed statistically	Returned surfaces, ground-based optical and radar measurements	Unknown

In LEO, a cloud of debris becomes randomized in argument of perigee and right ascension of ascending node within a few months or years after creation. Couple of weeks after breakup, the debris can be seen as densely packed in hundreds of thousands of fragments larger than 1mm. If these debris pass through the orbit of a space asset (e.g. International Space Station), they could present a high probability of collision. Engineering models are designed to provide accurate results in a timely fashion, the debris environment that will be encountered by a spacecraft in the present and near-future (i.e. on time-scale of decades). The generation of these space debris are observed from manned and unmanned spacecraft as shown in Fig. 1.3.

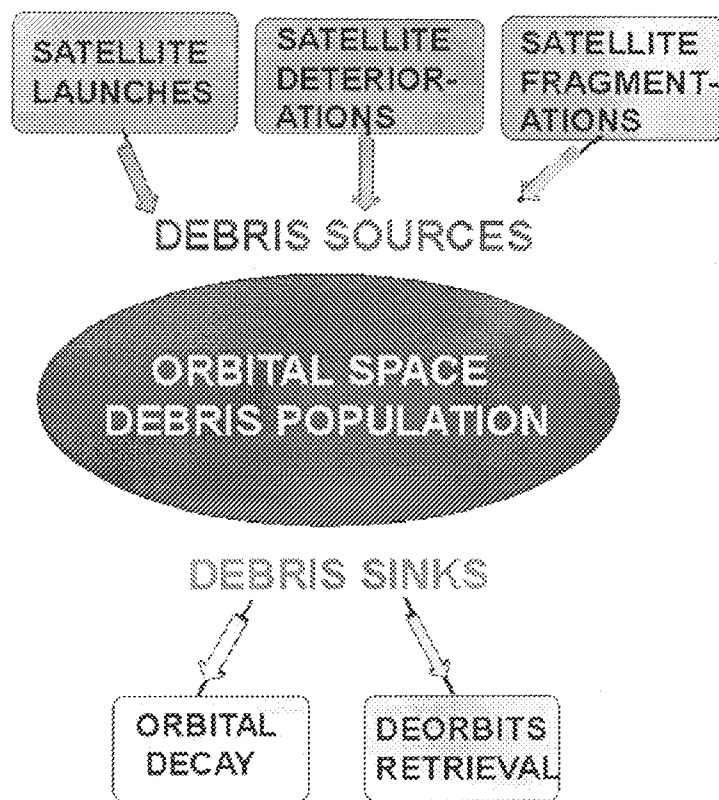


Fig. 1.3: Space Debris generation [Bariteau, 2002].

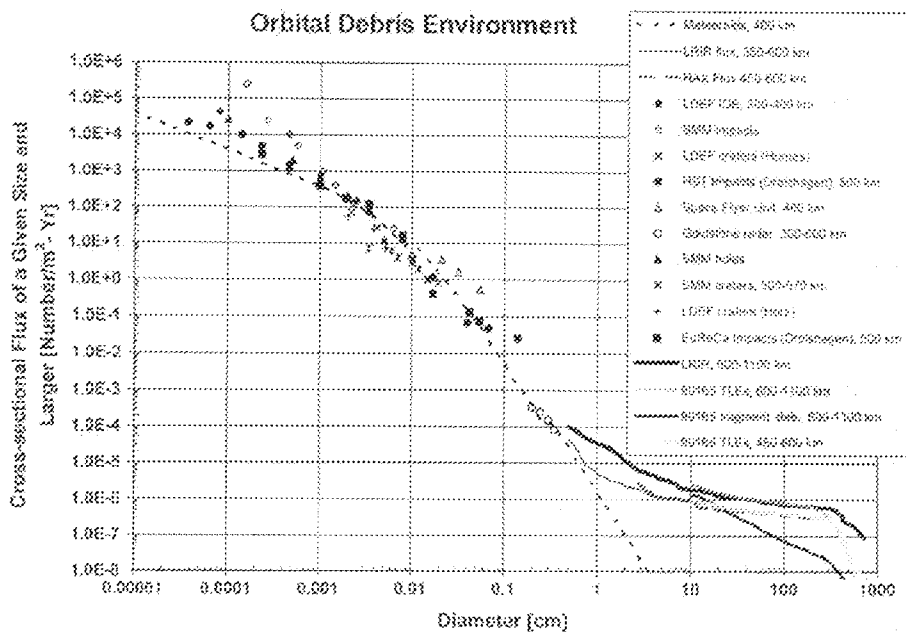


Fig. 1.4: Plot of Debris Flux versus Diameter as Determined by Multiple Instruments and Studies [Johnson *et al.*, 2004]

1.3 Effects of Debris on Space environment

The space environment is clouded with debris of different sizes and mass and the effects on the space assets are observed in four categories of space system operations such as period of in- orbit, projected orbital slot for new launch, orbital altitude and orbital inclination. The debris effect on the launch and operation of satellites is dependent on the size of the debris (large or small).

1.3.1 Effects of Large Debris

Large debris objects are typically defined as objects larger than 10 cm in size and such objects are capable of being tracked, and orbital elements are easily maintained along their orbiting planes. An example of such effect is during the course of shuttle missions, where International Space Station (ISS) crew executes collision avoidance maneuvers in order to

avoid catastrophic collisions with a large debris object. The large debris collision is capable of total break-up of a functional satellite in orbit. Another instance was recorded of two unmanned satellites to have performed collision-avoidance maneuvers to avoid large debris; these are the European Remote Sensing satellite (ERS-1) in June 1997 and March 1998, and Satellite Pour l'observation de la Terre (SPOT-2) in July 1997 [Megan, 2009].

The effect of collision-avoidance maneuvers is that more fuel may be expended during Launch Early Orbit Phase (LEOP) both in satellite altitude and inclination determination. Also, in-orbit operation of a satellite collision-avoidance maneuvers results in shorter lifespan against its original design life. This occurred in the post-processing of orbital parameters, which indicates that one of the predicted collisions would have actually occurred. However, owners of such satellite may want to increase the safety distance between the objects because of positional uncertainties, which will likely reduce the fuel budget of the satellite.

1.3.2 Effects of Small Debris

Small debris objects (smaller than a few millimeters in diameter) have caused damages to operational space systems. This damage can be divided into two categories as damage to satellite surfaces and subsystems, which affects the system operations of an in-orbit satellite. The categorization of the effects of small debris is as listed:

- (a)* Damage to shuttle windows and high gain antenna
- (b)* Severing of the Small Expendable Deployer System-2 (SEDS-2) tether
- (c)* Damage to other exposed shuttle surfaces

(a) and (b) are damages due to space debris but it is unclear whether (c) is caused by man-made debris or a micrometeoroid. Other effects are when astronomers are observing objects in space during wide field imaging, which also increases the number of trails per plate caused by small debris. These trails degrade the quality of the observations. Space debris trailing will entirely negate a photometric observation when debris crosses the narrow photometric field.

1.3.3 Debris Collision Impact

Collisions which can be termed 'catastrophic' are the result of a complete fragmentation of impactor and target (when impactor mass is smaller than target mass by definition). This has been shown to occur empirically when the impact energy per target mass exceeds 40 J/g. In order to avoid collision with debris during flight, operational procedures have been adopted. In the case of the Space Shuttle, the orbiter is often oriented during flight with the tail pointed in the direction of the velocity vector and such flight orientation was adopted to protect the crew and sensitive orbiter systems from damage caused by collision of space debris.

1.4 Statement of the Problem

The phenomenon of space debris has drawn attention of the space fairing nations to observe that:

1. The Earth orbit congestion is becoming a threat to spacecraft launch and other explorations and requires an address
2. The records of space debris falling on Earth have accounted for some human accidents which require urgent attention.

This global problem of the space environment congestion with space debris creation in both near and far orbits require address. It is noteworthy that Nigeria has also, in her bid to join the space fairing nations contributed to the number of space debris with the loss of NigComSat-1 in November, 2008 and NigeriaSat-1 at its end of design life in 2008. This thesis titled is aimed to provide mitigation technique and evacuation of space debris for a cleaner space environment.

1.5 Aim and Objectives

The aim of this thesis is to reduce the congestion of dead satellites fragments and other space debris (in the region of 10 μ m to 10cm) in near Earth orbits through "Modelling of Electromagnetic Debris in Space by an Evacuator". The objectives of this work are stated below:

1. The discussion of the model result is aimed at mitigation of space debris generation.
2. Promotion of cleaner orbital slots for present and future use and for safe environment on Earth.

1.6 Methodology

This thesis, "Modelling of Electromagnetic Debris in Space by an Evacuator", examines the behaviour of satellites after their end of life and other debris resulting from collisions and their removal to avoid collision with operational satellites. These dead satellites in uncertain orbits, after end of life are called space debris. The modelling of an electromagnetic payload will enhance the de-orbiting of the remains of the dead satellites.

The main payload, the space debris evacuator, would be an electromagnetic system which, when switched on, will generate fluxes to attract nearest satellite debris with respect to mass and size and maneuvering it to re-enter low orbits. Then when the circuit is switched off, the magnetic circuit releases its hold on the satellite debris, thereby reducing the period of orbiting object before entering into the Earth under a tracking system. The payload is integrated into the platform of a typical satellite. The solution provided in this thesis is a simple model of satellite debris evacuation system.

CHAPTER TWO

2.0 LITERATURE REVIEW

Space and Satellite debris phenomenon became a subject of importance when astronomical studies discovered some bodies passing through the near-Earth space. These objects are smaller and more difficult to observe because some are dark and some are like stars but burning out so fast. These are called the *Asteroids*, *Meteoroids* and *Comets*. Also, spacecrafts that have reached their end of life, failed spacecraft during launch, fall-off fairing, rocket boosters and stages, paint flakes all constitute what is called space debris [Bariteau, 2002].

At a United Nations meeting, the item on space debris was included in the agenda of the Scientific and Technical Subcommittee at its thirty-first session of February 1994, in accordance with General Assembly resolution 48/39 of 10 December 1993. This Subcommittee, at its thirty-first session, expressed its satisfaction to have the subject of space debris as a separate agenda item after many years of discussion in various international fora, including the Subcommittee and the Committee on the Peaceful Uses of Outer Space (COPUOS). The Subcommittee agreed that consideration of space debris was important and that international cooperation was needed to evolve appropriate and affordable strategies to minimize the potential impact of space debris on future space missions. At its subsequent sessions, the Subcommittee continued its consideration of that agenda item on a priority basis [Timothy et al, 2003]

Space-faring nations agreed that the outer space, especially the near-Earth orbit, has become increasingly populated with man-made junk. These are space debris which are inevitable consequences of the global uses of space, emanating from every single space launch which creates one form of debris or the other. One thing that is certain is that failure to stem the creation of space debris will undercut the security of all assets in space, increasing the likelihood of collisions and possible conflict over liability for them. Therefore, this act tends to undermine the UN goals of peaceful use of outer space for socio-economic development as litigation could arise from collision problems [United Nations, 1999].

The official catalog of space objects kept by the U.S. Air Force's Space Surveillance Network (SSN) contains about 9,000 objects, but the Air Force also tracks another 4,000 objects whose origins and exact orbits are not yet confirmed. Although there is no unclassified, publicly available data on exact number of operational satellites orbiting the Earth at any time, U.S. officials said that only about 6 percent of 13,000 objects being observed are working satellites or spacecraft (such as the International Space Station). The rest is debris. A study of debris distribution reveals the near-term troubled zone to be a spherically symmetric region between the altitudes of 700 km and 900 km. One immediate reason for increased interest in orbital safety and categorization is the February 10, 2009 collision of the Indian-33 satellite with the defunct Russian Cosmos 2251 satellite [Megan, 2009].

That collision created more than 800 pieces of debris 10 cm in length or above, in two clouds. Over time, these two clouds would slowly expand outward, threatening other working satellites that move in nearby orbits. Because the destroyed Indian satellite flew

in a near polar orbit, debris from this collision now poses an additional hazard to some remote sensing satellites. NASA was able to accomplish this observation because their experts have access to the classified database of satellite orbital positions maintained by the U.S. Air Force [Megan, 2009]. The classification of space debris observed by U.S. Air Force is shown in Fig. 2.1.

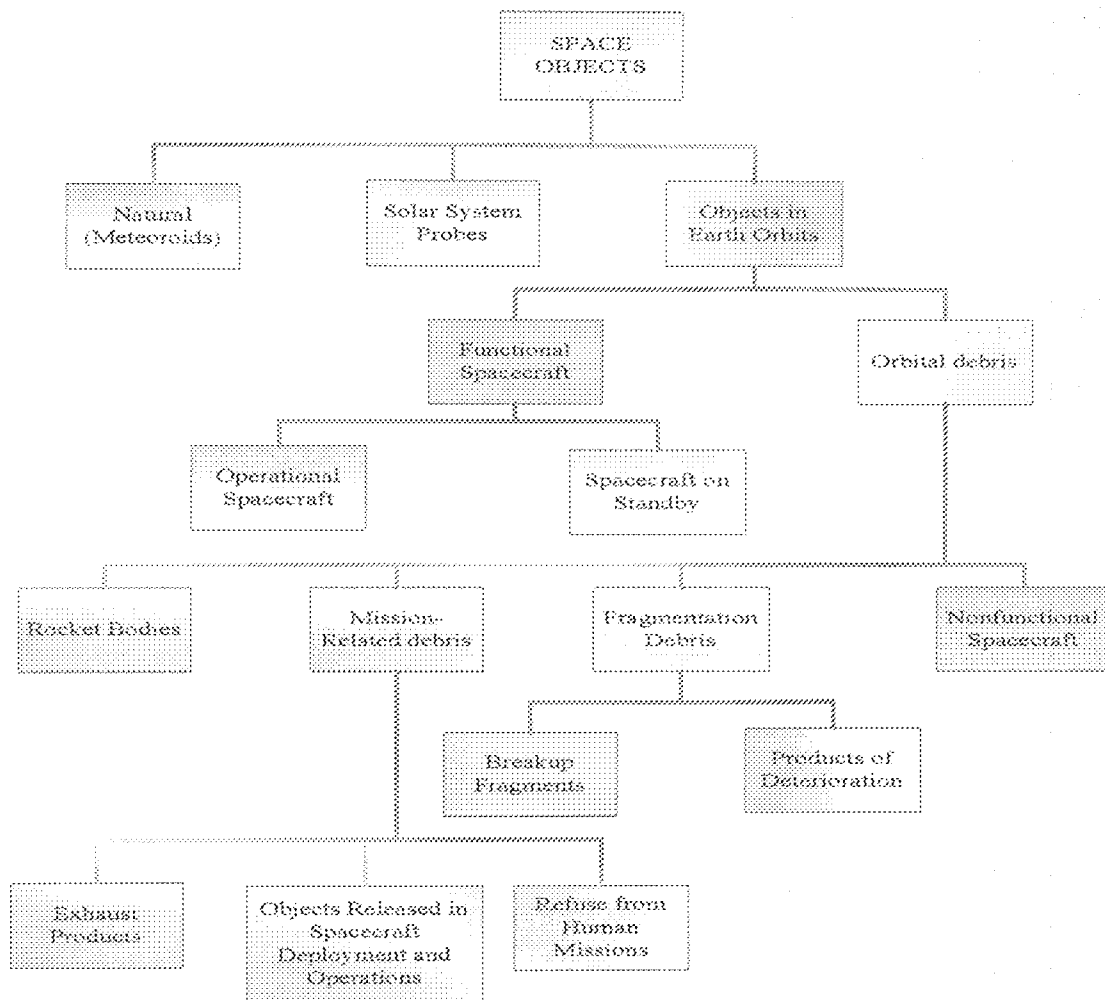


Fig. 2.1 Classes of space objects [United Nations, 1999].

The collection of recent functional and non-functional satellites in a graphical plot against the different orbital slots showed that orbits in 1,400 – 1,500 km range have the highest objects of about 460 spacecraft as shown in the graph Fig 2.2.

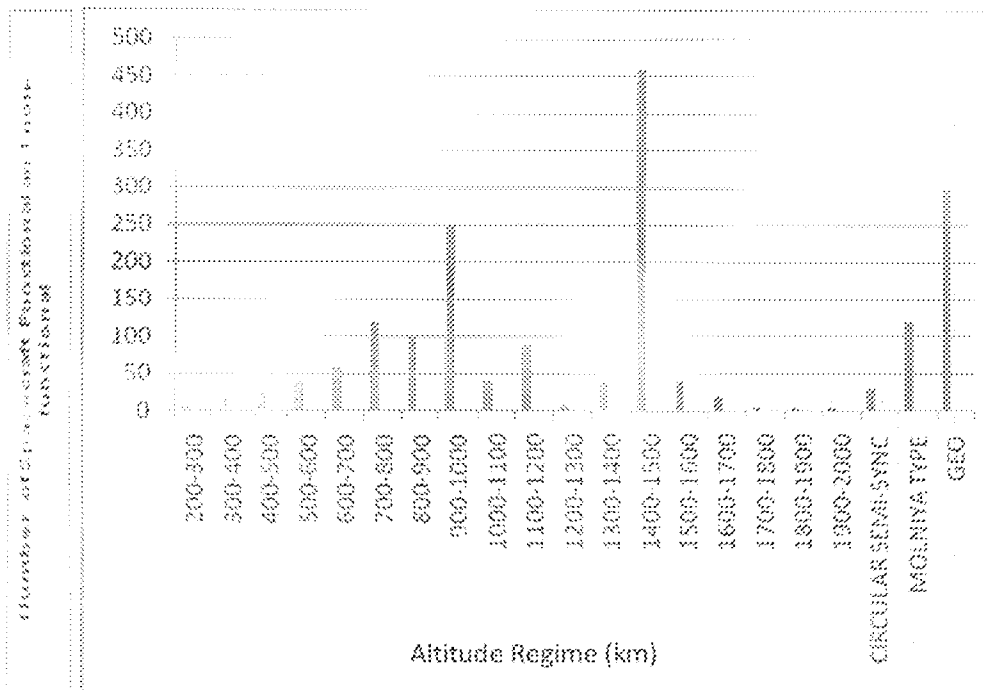


Fig. 2.2: Recent satellites and their orbits [Inter-Agency Space Debris Coordination Committee, 2003]

Space scientists estimate that there are more than 100,000 objects between 10 cm and 1 m in size and perhaps trillions of pieces yet smaller [Johnson *et al*, 2004]. Space debris is concentrated in the orbits most useful for human space operations in Low Earth Orbit (LEO - defined between the Earth's atmosphere from 100 km to 2,000 km in altitude) and in Geosynchronous Earth Orbit (GEO, roughly 36,000 km above the Earth where satellites essentially remain stationary over one spot on the ground). It is much easier to prevent space debris than to clean it up. Indeed, there are currently no technologies that can reliably "clean up" space junk in decades past. Although preventing the creation of debris may be simpler than removal, nevertheless it is not exactly easy as it requires operators to incorporate special design features into their spacecraft or satellites. Nonetheless, many space-faring nations and commercial interests have woken up to the need for debris

space-faring nations and commercial interests have woken up to the need for debris mitigation due to concerns that if nothing is done now, certainly useful orbital planes may no longer be safe for satellites and spacecraft. This necessitates the action by UN on mitigation of the debris.

2.1 Examples of Damages Caused by Space Debris

Space Debris are potential threat to space missions. Also they can be a danger to people and things on the ground, as some space junk in LEO will eventually de-orbit, pass through the atmosphere and land, thus possibly causing human accidents in farm lands and/or to fishermen when they fall into the ocean. Although such land and sea falls are rare, they do happen when very large space objects de-orbit.

Few examples of space debris accident and damages are;

- i. NASA replacement of two Space Shuttle windows after each mission due to damage by small pieces of debris as quoted by Joseph Loftus – former Assistant Director of Engineering for NASA’s Space and Life Science Directorate.
- ii. Record of large pieces of Skylab falling over Western Australia in July 1979.
- iii. Pieces of Delta 2, second stage rocket falling over Cape Town, South Africa in April 2000.
- iv. The fairing of Telesat Anik F falling in 2005 at Columbia.

The height of the need for mitigation of space debris in recent time is the collision of American and Russian satellites on Friday 13th February, 2009. The numbers of debris

added to space are not yet determined but continue to pose problems for space missions [United Nations, 1999].

2.2 United Nations Intervention Programme for Space Debris Mitigation

An Inter-Agency Space Debris Coordination Committee (IADC) was formed in 1993 with the primary purpose to exchange information on space debris research activities between member space agencies, to facilitate opportunities for cooperation in space debris research, to review the progress of ongoing cooperative activities, and to identify debris mitigation options [United Nations, 1999].

The scope of IADC includes:

- a. to review all ongoing cooperative space debris research activities between member organizations;
- b. to recommend new opportunities for cooperation;
- c. to serve as the primary means for exchanging information and plans concerning orbital debris research activities;
- d. to identify and evaluate options for debris mitigation.

The membership of the IADC was drawn from the

1. Italian Space Agency (ASI),
2. British National Space Centre (BNSC),
3. Centre National d'Etudes Spatiales (CNES),
4. China National Space Administration (CNSA),
5. Deutsches Zentrum für Luft- und Raumfahrt e.V. (DLR),

6. European Space Agency (ESA),
7. Indian Space Research Organisation (ISRO),
8. Japan Aerospace Exploration Agency (JAXA),
9. National Aeronautics and Space Administration (NASA),
10. National Space Agency of the Ukraine (NSAU) and
11. Russian Federal Space Agency (ROSCOSMOS).

Other organizations or government agencies are welcome for research presentations on space debris mitigation [IADC, 2003].

Among other things, the IADC work frame includes;

1. Measurements of sizes of space debris.
2. Identification of environment and collection of database of space debris.
3. Protection of operational satellites and astronauts.
4. Mitigation of space debris.

2.3 Review of Past Efforts

After the establishment of the IADC, member nations and agencies began to conduct researches and present papers in conferences, and recommendations are being made at the COUPUS meetings based on the terms of reference given to them. Database of space debris environment modelling and evacuator designs are also being presented as listed below:

- i. Natural Mechanism
- ii. Laser Model
- iii. Electro-dynamic Tether for Active Debris Removal

- iv. Generic Inflatable De-Orbit Device (iDod)
- v. Space shuttle evacuator

2.3.1 Natural Mechanism

A satellite in the LEO takes an average of 4-6 hours to revolve round the Earth, and about 12 hours in the MEO depending on the altitude (height). It is 24 hours for satellite in the GEO orbits, which makes it geostationary with respect to the Earth rotation around the sun. Also, the velocity of the satellite reduces as the height of the orbit increases such that the velocity in the geostationary orbit is about 3 km/second (11,000 km/hour). Satellites at these orbits and velocities naturally revolve round the earth while in operational life [Breukelen et al. 2006]. These satellites began to drift with change in velocity caused by air-drag perturbation, as they get to end of life, thereby becoming debris. Since the rate of removal of debris by natural mechanisms, such as air-drag perturbations, is exceeded by the rate of spacecraft deposition in space the orbits are still crowded with debris.

Basically, operators should de-orbit their low-Earth-orbit spacecraft such that they will burn up in the atmosphere, or splash down in uninhabited ocean areas. This natural de-orbiting is unguided and may cause accident if the fall is recorded in residential area, and could result in displacement of fish farmers or disruption of vessel operation on the high sea. In the case of telecommunication and other satellites operating in the commercially-valuable geostationary zone, they boost their satellites to a safe disposal orbit which must be about 150 to 300 km further away from the GEO orbits and the satellites in such orbits naturally orbit the Earth forever [Timothy et al. 2003].

and operational time and, therefore, increase cost of satellite building and operation. In the commercial world, it has affected competitiveness and there is an international consensus to accept such costs [Springer, 2006]. The possible damages in natural mechanism model from booster fall off and decay of satellite orbits have not provided an amicable mitigation measure.

The problem with natural mechanisms is the long duration of decay of orbits and eventual de-orbiting of the space debris, leaving room for possible collisions and defragmentation in the orbits [United Nations, 1999].

2.3.2 Laser Model

Another model of debris mitigation is to have an in-situ laser on board a craft, such as the International Space Station (ISS), which would essentially work the same way as a ground-based laser, but would have the added benefit of being much closer to the actual debris. Though several methodologies have been developed, the most feasible seems to be a ground-based laser system that would hunt down space junk and shine its laser at the particle for several minutes. The energy of the laser light would actually set ablaze a tiny layer on the debris surface, thus creating a thrust for the object as the molecules in the thin layer expand away from the object while they are being vaporized [Theresa, 2004].

The most well-known of these projects is the Orion Project, a major study which began in the late 1970s, and which continues to undergo development with help from NASA and other government agencies. The focus of Orion has been to look at the possibility of using high-powered laser light beams to actually deflect orbital debris out of the way of spacecraft and into the Earth's atmosphere, where it can burn up.

high-powered laser light beams to actually deflect orbital debris out of the way of spacecraft and into the Earth's atmosphere, where it can burn up.

The study of this model showed that the operation in orbit is theoretically possible; but from a systems development management point of view, it is not very practical, as being criticized by other researchers. Accordingly, scientists and engineers are working primarily on the former Orion model, and are hopeful they will soon get to test out the concept using a special laser system. In justifying the study, Campbell – a Scientist said “if we can demonstrate that we can detect a tennis-ball-sized object 2 kilometers (1.2 miles) away, and we can hold a laser beam on it through turbulent atmosphere, then that should be enough to prove to even the greatest skeptics that this is something that can be done” [Theresa, 2004].

However, two major problems with this model suggest the approach would never work because, the system would take more power than the entire space station has and humans would not have enough time to detect and hunt down an object coming over the horizon before it either hits or passes the craft. Also, the vapourized particle would increase the population of tiny space debris.

2.3.3 Electro-dynamic Tether for Active Debris Removal

In the continuous efforts and study of space debris mitigation, the Inter-Agency Space Debris Coordination Committee (IADC) under the Agency of the Japan Aerospace Exploration Agency (JAXA) had conducted the study on potential benefits and risks of using Electro-dynamic Tethers for End-of-life De-orbiting of LEO Spacecraft. The procedure of the model showed that a tether strand is thin but long enough to have a large

equally spaced loops. This has been suggested as one of the promising models [Vannaroni *et al.*, 2000].

The Kyushu University developed a mathematical model, evaluating the survival probability of the double tether system. Kyushu University has extended the aforementioned mathematical model after the completion of the first study. The resulting model can provide the maximum mission success rate that a double tether system with a finite clearance can attain regardless the number of loops. Kyushu University is applying this new model to evaluate the mission success rate of an electro-dynamic tether system [Vannaroni *et al.*, 2000].

The objective of this research and development of an electro-dynamic tether system was to reduce the orbital lifetime of spacecraft as being conducted. The system is an advanced propulsion technology that uses no propellant or working gases, in principle. Because debris de-orbit systems require highly efficient propulsion systems, the system is an attractive model. The work of this simple electro-dynamic tether system is being conducted with the intention of eventual demonstration. The procedure is by generation of thrust, and is achieved by equipping a tether longer than one km and an electron emitter with emission capability of over several hundred milliamps.

In addition, electrostatic and magnetic probes and GPS receivers are used for investigating the efficiency and the system behavior in orbit. Changes in the in-plane libration angle of the tether with and without control using GPS shows that GPS information is useful to control the tether attitude, even though the information includes a certain level of measurement error. The laboratory trial-and-error fabrication and testing of bare tethers

the tether with and without control using GPS shows that GPS information is useful to control the tether attitude, even though the information includes a certain level of measurement error. The laboratory trial-and-error fabrication and testing of bare tethers has been performed. The tether functions as an electron collector, a power source (i.e. generating electromotive force), and a thrust generator in the system. In these tethers, aluminum wires and carbon fibers are braided or twisted to impart strength, flexibility, and electric conductivity [Vannaroni et al, 2000]. The limitation of this system is that, because the generation of thrust by the system has not been demonstrated in space, it is indispensable to perform in-orbit experiments in the near future.

2.3.4 Generic Inflatable De-Orbit Device (iDoD)

The university dons at the Faculty of Aerospace Engineering, Delft University of Technology, Netherlands, and experts in Space Systems Engineering, developed a model of a flexible connector piece which is constructed of five inflatable tubes. The generic inflatable construction has a stowage and deployment of the inflatable structure. The design outlined the concept and preliminary of a generic inflatable de-orbit device, which reduces the ballistic coefficient of the satellite by increasing its frontal surface area. The device is of the attached ballute type and consists of a thin membrane covering an inflatable structure, which is chemically rigidized after deployment. New space debris mitigation guidelines require satellites in low Earth orbit to de-orbit within 25 years after end of life. This effectively limits the orbital altitude of conventional satellites to 400-700 km. For satellites employing the generic inflatable de-orbit device discussed here, this range is extended to at least 900 km for the same de-orbit period of 25 years after end of life [Walker et al, 2000].

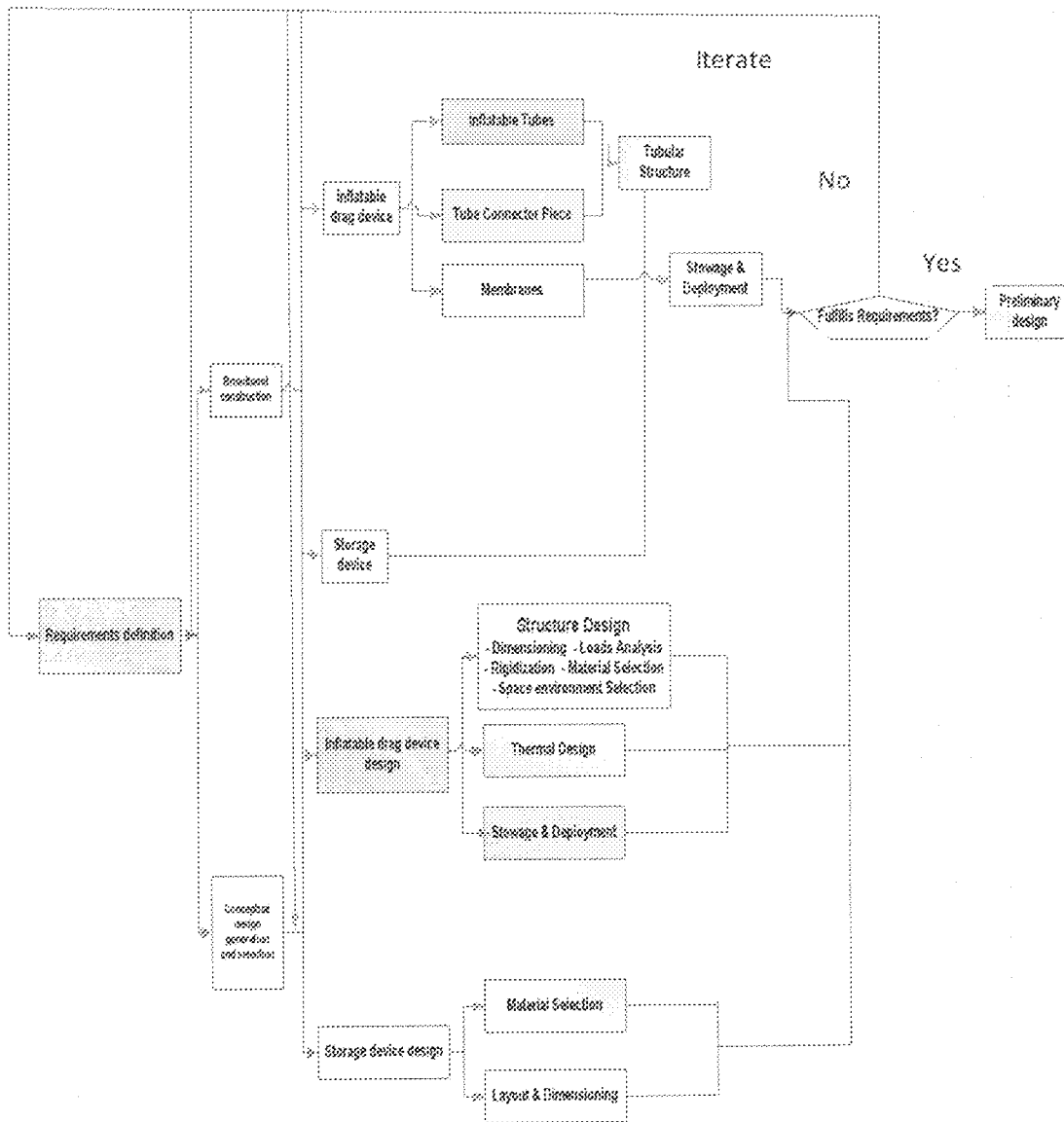


Fig. 2.3: iDod design process [Walker *et al.*, 2000].

The iDod presents the development of an inflatable De-orbit device (iDod), which offers a significant reduction in de-orbit time while limiting the expense in terms of mass and volume. The presentation showed that increasing the drag encountered by a satellite results in an increased deceleration, and hence an increase in orbit decay rate. The drag

increase is obtained by increasing the drag area A of the satellite. This leads to a decrease of the ballistic coefficient C_B of the satellite which is given by the equation;

$$C_B = \frac{m}{C_D A} \quad (1.1)$$

C_D is the drag coefficient of the satellite and m is the mass of the satellite. In iDod study by D.C. Maessen, C_D is 2 and $m = 1$ kg. The drag area of a freely rotating 1-unit satellite is 0.015 m^2 , resulting in $C_B = 33.3 \text{ kg/m}^2$ [Walker *et al*, 2000].

For instance, an orbit lifetime analysis has been performed with Satellite Tool Kit (STK)

7.0.1. Results are given in Table 2.1.

Table 2.1: Values for drag area and ballistic coefficient [Walker *et al*, 2000].

	Orbit 1	Orbit 2	Orbit 3
Drag Area [m^2]	0.015	0.15	0.30
Ballistic coefficient	33.3	3.33	1.6
Orbit initial altitude [km]	700	900	1000

The analysis indicates the requirement to de-orbit a 1-unit satellite by natural orbit decay within 25 years after EOL from a circular orbit with given initial altitude. The details of the study shown in the Fig. 2.4 describe that the orbit decay increases in an exponential manner.

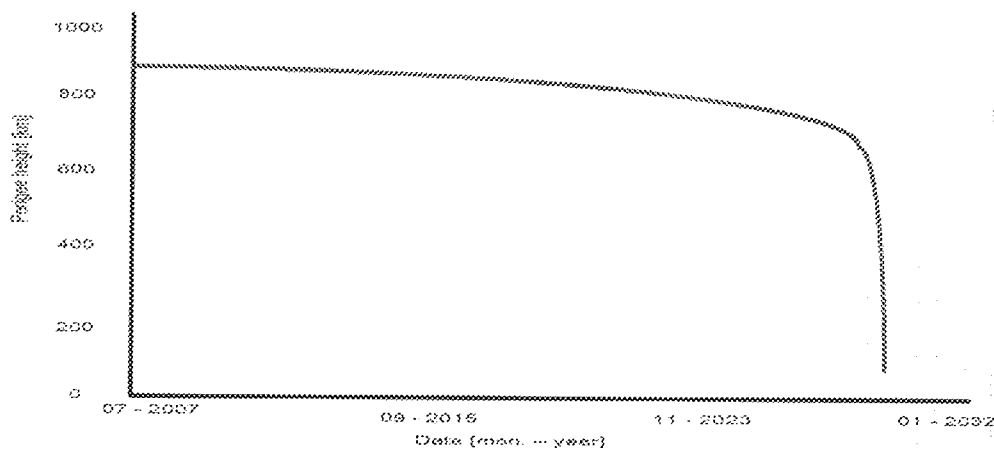


Fig. 2.4 STK de-orbit prediction [Walker *et al.*, 2000].

The increase in orbit decay rate is logical, since the atmospheric density, the factor influencing orbit decay rate the most, decreases exponentially with increasing altitude. Without iDod system, de-orbiting for the satellites in about 700 km attitude takes 197 years. This has drawn attention to the area-time product (a measure for the probability that space debris impacts on a satellite) of the satellite.

The iDod took cognizance of stability for maximum material efficiency, the inflatable structure was made to be a flat plate oriented perpendicular to the velocity vector of the satellite. However, there are several natural causes that result in disturbance torques which affect the orientation of the satellite. Among these are:

- Aerodynamic drag
- Solar radiation pressure
- Magnetic field of the Earth
- Gravity gradient

Ideally, the orientation of the satellite with deployed inflatable is passively stabilized and dictated by aerodynamic drag. The concept of the iDod is a pyramid structure as shown in

Plate V and the description of storage in Plate VI. The structure demonstrates how one unit of satellite is inflated by the pyramid device, which is capable of dragging the one unit satellite to a low Earth orbit for final de-orbiting.

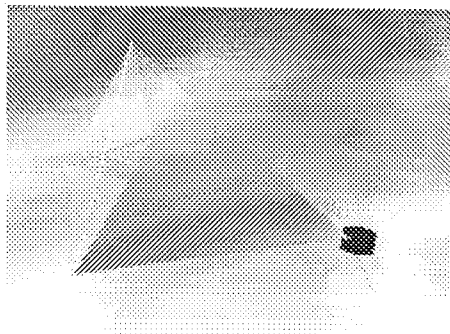


Plate V: Pyramid concept [Maessen, 2006]

The inflatable drag device is stowed inside an aluminum storage device. The flanges and the lid of the storage device replace a standard satellite shear panel. The dimensions of the storage device allow it to be slid inside standard satellite of a Cube-form Satellite frames. The small height of the storage device leaves about 8 cm of height for Programmable Circuit Board (PCB) and other components to be stacked inside the Cube-form Satellite as shown in Plate VI.

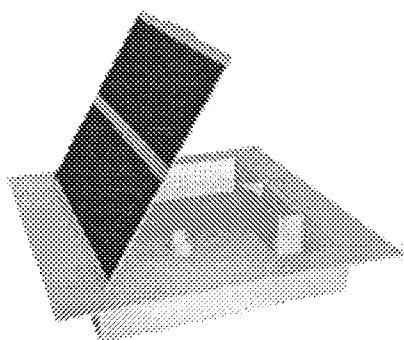


Plate VI: iDod storage device [Maessen, 2006]

The lid of the storage device is rotated around an axle by means of helical torsion springs. A string wire holds down the lid and is melted through by means of a resistor once the lid

needs to be opened. The membranes and tubes of the inflatable structure are folded separately. Once folded, the membranes are connected to the tubes. Separate folding allows the membranes to be folded into small packages, which results in a high packing efficiency. Deployment of the inflatable structure is achieved by pressurizing the tubes of the inflatable using nitrogen gas. This gas is stored in solid form and produced at ambient temperature by means of a Cool Gas Generator (CGG). Production of all inflation gas, 0.12 normal litres, is performed in one second. This is very fast and its influence on the deployment of the inflatable needs to be determined.

The deployment tests for breadboard inflatable structures indicate that deployment occurs in three steps: First, the central tube fully deploys. Then, the spokes deploy up to approximately half their length and the membranes are deployed in length-direction. Finally, the remaining half of the spokes inflates and the membranes deploy in width-direction. The work showed that the model of the iDoD has been developed confirming the proper deployment of the inflatable structure as well as the packing efficiency of 20%. To enable operational satellites to take evasive actions in time, the inflatable structure can be metalized thereby increasing the visibility on radar [Breukelen, 2006].

The limitation of the iDoD shows the drag augmentation using an inflatable structure with obvious benefit of shielding the satellite from strange objects, it is not certain whether the area per altitude of the satellite is a proper measure for determining the desirability of using inflatable structures for orbit decay purposes.

2.3.5 Space Shuttle Evacuator

The most critical way to reduce space junk is to send less of it up in the first place. Currently about 200 objects per year are added to the space environment around the Earth. And with more and more emphasis placed on space business and science, it seems likely that the upward trend toward more space debris will only increase.

Currently, NASA and other members of the international space community are trying to fight space junk by keeping the debris in check as much as possible. Already, there are a number of design requirements and procedures for each launch and space mission that ensure the least amount of space junk, including controlled de-orbiting of aging spacecraft. One of the attempts was the launch of a shuttle to pick up a satellite at end of life, but the exercise was found out to be too expensive. Other model being developed is the drag net, similar to iDod, which can be released like a parachute. The limitations are the method of discharge of the captured debris, dimension of the net, possible collision and further creation of smaller debris. The major limitation of space shuttle evacuator was cost but it is an important medium of evacuation of accidental spacecrafts near the earth orbits [Theresa, 2004].

2.3.6 Proposed Electromagnetic Space Debris Evacuator

All the past efforts on space debris mitigation reviewed in this study posed a good concept but have not been practicable except the Generic Inflatable De-Orbit Device (iDoD), which is a self de-orbit concept. The iDoD concept is capable of reducing the orbit re-entry period and is typical for the near Earth orbit satellites. This thesis on Electro-Magnetic debris evacuation is modelled to simulate the evacuation of ionized particles of dead satellites, other space debris in near-Earth orbits and other unwanted space objects

(asteroids and meteoroids) in the size range of 10 μ m to 10cm. The Electro-Magnetic module forms the main payload of the spacecraft, which the operation targets for the evacuation of space debris. The detailed description of the modelling and operation is enumerated in Chapter Three.

CHAPTER THREE

3.0 MATERIAL AND METHODS

The concern of space orbit population with objects and rocket pieces has continuously been on the increase and several efforts are being made to curtail the menace. This thesis provides a solution for the removal of the space debris from the near-Earth (e.g. LEO) orbits using an electro-magnetic evacuator, whose block diagram is shown in Fig. 3.1.

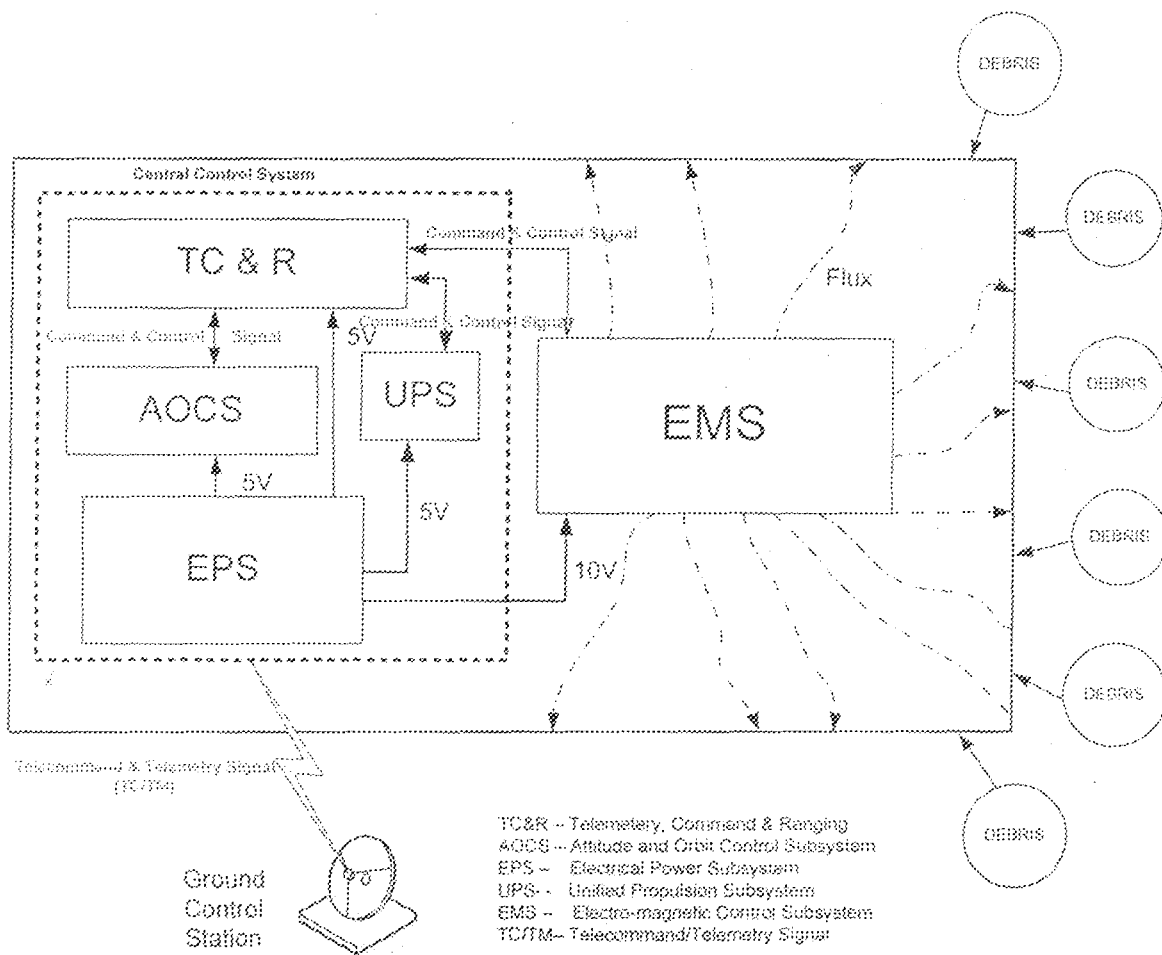


Fig. 3.1: Space Debris Evacuator Block Diagram

The block diagram indicates the signal flow within the space debris evacuator. The labelled blocks are described as follows:

- AOCS is the onboard Attitude and Orbit Control of the evacuator for orientation and attitude
- EPS is the electrical power supply, which is a bank of batteries supported by solar panel during sunlight
- TC&R is the subsystem for the tracking and ranging control of the evacuator in orbit
- UPS is the universal propulsion subsystem, which supplies the fuel for maneuvering the evacuator during orbit operation and near-Earth re-entry.
- EMS is the main payload of the spacecraft (the Debris Evacuator) and draws voltage from the EPS to generate electro-magnetic flux fields described in the block diagram.
- TC/TM is the Telecommand/Telemetry signal

The applied voltages (5 V and 10 V) are typical of the NigComSat-1 satellite, since a typical spacecraft platform is adopted for the development of the debris evacuator. This thesis is focusing on the removal of space debris in the size range of 10 μm to 10 cm diameter and a mass of approximately 15 to 150 milligrams

Hence, the generated fluxes drag the debris in this range of sizes and mass. The developed debris evacuator is targeted towards this group of debris, which populated the useful orbits. The applied voltage to the EMS generated fluxes hold the space debris onto the

evacuator until the near-Earth re-entry. The re-entry of the space debris evacuator, after it might have completed its mission, is by commands sent from the ground control station to the spacecraft (debris evacuator) to re-enter the Earth's atmosphere where it discharges the debris in a predetermined safe zone (ocean or desert). The recovery of the debris evacuator and its re-launch is a subject of further study. This is also typical of the manned mission Earth re-entry. Fig. 3.2 illustrates the developed debris evacuator in its orbit with attracted space debris and the ground control station for its maneuvering operation.

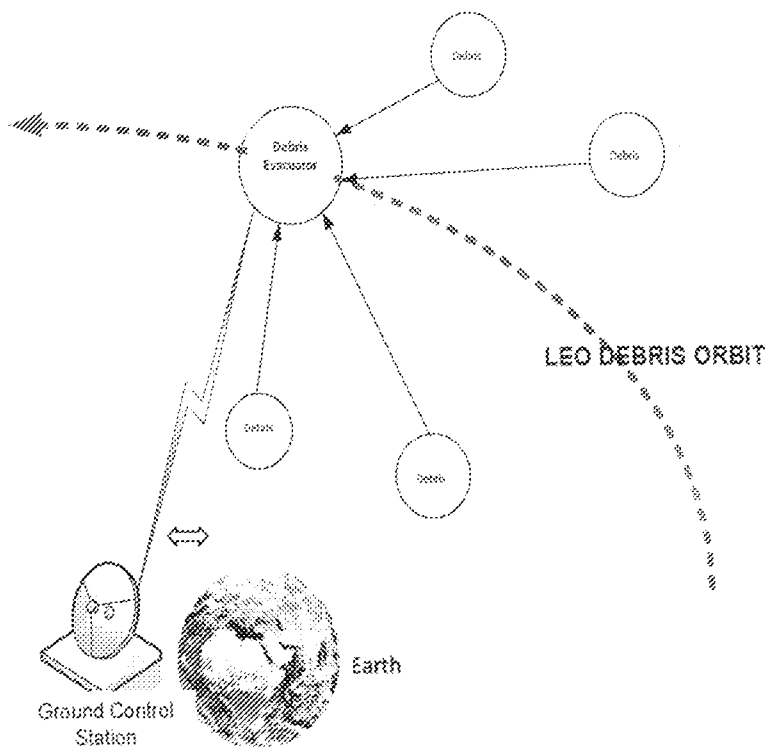


Fig. 3.2: Illustration of Debris Evacuator and Attracted Space Debris in Orbit.

3.1 The Features and Integration of Electromagnetic Evacuator Model

The space debris evacuator model developed is shown in Fig. 3.3. It adopts the structure of a regular spacecraft with its payload as the electromagnetic circuit integrated to the platform/bus and other ancillary controls and subsystems. The electromagnetic winding is

on the four panels (East, West, North and South) of the satellite platform. The Earth panel (Y) in the figure carries the satellite stabilization boom and bank of batteries, while the anti-Earth panel (X) carries the solar panel as source of power supply and charging of the on-board batteries. The central cylinder carries the propellant tank used for the evacuator launch and maneuvering during the evacuator's lifetime.

The magnetic core selected for the developed debris evacuator is a ferrite of "nickel zinc (NdFeB)" because of its low reluctance to flux generation, having a permeability of $1.05\mu_0$ where μ_0 is the permeability of free space (i.e. $4\pi \times 10^{-7}$ H/m).

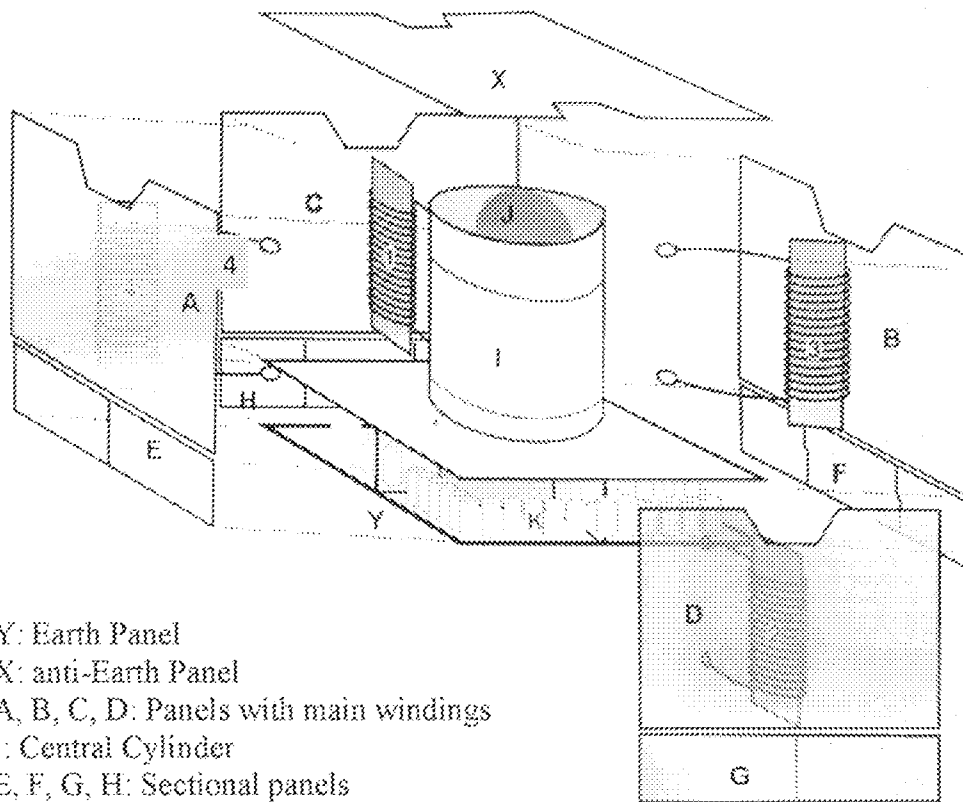


Fig 3.3: Configuration of the Developed Electromagnetic Space Debris Evacuator

Panels A, B, C and D are made of aluminum alloy, and are coupled with the magnetic core (ferrite of nickel zinc) that carries the coil windings to produce electro-magnetic flux

required in the integration. The aluminum alloy is used because of its low mass and tendency to generate charged ions with applied magnetomotive force. The strip panels (Nickel Zinc) labelled 1, 2, 3 and 4 are the magnetic core with 16 coil windings each. The windings are connected in parallel to the battery to ensure that at least one or two magnetic windings are connected at any time for flux generation especially in case of circuit breakdown in the developed debris evacuator. The lower panel *Y* (Earth deck) carries the stabilization boom and battery bank (labelled *K*), which powers the evacuator during eclipse. The battery bank is covered by the lower panels labeled *E*, *F*, *G* and *H*. The central cylinder *I* gives structural strength to the configuration. The anti-Earth panel *X* carries the solar panel, the primary source of power supply to the evacuator in space orbit. The four panels *A*, *B*, *C* and *D* are structured in matrix squared shape as shown in Fig 3.4 which illustrates the in-orbit configuration of the developed model of the debris evacuator. The panels are to withstand the surface impact of the flying debris during attraction by the debris evacuator.

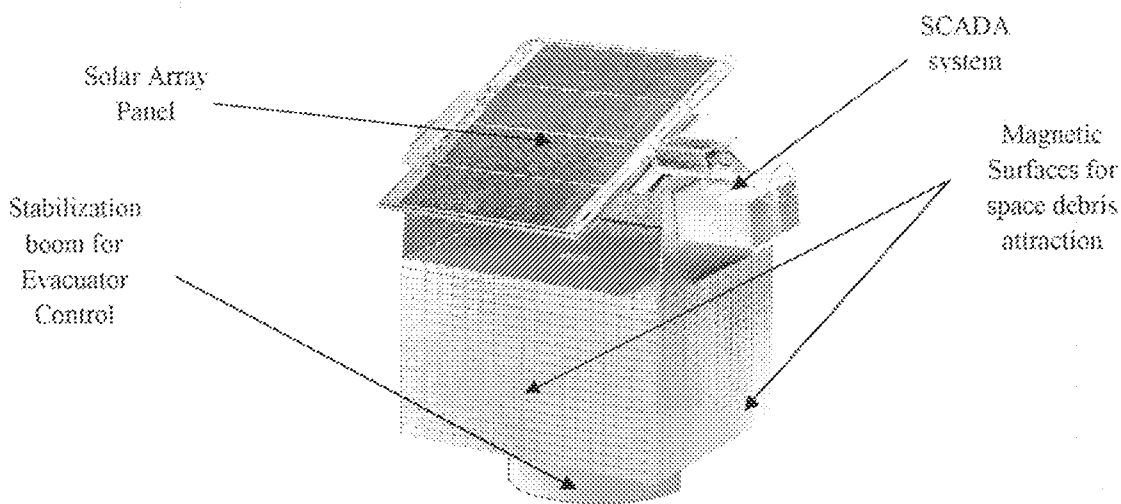


Fig. 3.4: In-orbit Configuration of the Developed Model of Debris Evacuator

The central boom is responsible for the stabilization and control of the evacuator while in orbit. A satellite operational mode with boom deployment status is one of the most

The central boom is responsible for the stabilization and control of the evacuator while in orbit. A satellite operational mode with boom deployment status is one of the most significant methods of attitude control. The satellite attitude is acquired from an attitude with the boom pointing towards Earth.

3.2 Mathematical Modelling of the Space Debris Evacuator Parameters

The mathematical modelling of the parameters of the space debris evacuator is shown in the following sub-sections.

3.2.1 Magnetomotive force in the Space Debris Evacuator

The microgravity experience in the outer space and the introduced electromagnetic fluxes follow the Ampere's law. In this thesis, an N -turn coil is wound round the magnetic core. This enables it to generate magnetic flux when current passes through the coil since magnetomotive force (like electromotive force in electric circuit) is directly proportional to the number of turns in the core as given in equation (3.1)

$$\Phi = FN \tag{3.1}$$

where

Φ = flux developed in the evacuator

F = magnetomotive force in the evacuator

N = number of turns of the coil in the evacuator

The coil of the debris evacuator is powered by the current generated from the solar panel to produce the flux which attracts the debris. The evacuator is installed with a detector sensor, which senses the nearest debris at a distance to the evacuator.

The magnetomotive force in the evacuator can also be expressed in terms of magnetic field strength and length of coil in the panel;

$$F = Hl \quad \text{[Ampere-Turns]} \quad (3.2)$$

where

F = Magnetomotive force developed in the evacuator

H = Magnetic field strength in the core of the evacuator

l = Length of the coil in the evacuator

The magnetomotive force developed in the debris evacuator resulting from the applied voltage produces the electromagnetic flux produced. The change in this flux is directly proportional to the number of windings and magnetic field strength of the core in the evacuator.

3.2.2 Electromagnetic Flux in the Space Debris Evacuator

The electromagnetic flux in the evacuator is expressed as

$$\Phi = BA \quad \text{[Weber]} \quad (3.3)$$

where

Φ = Electromagnetic Flux in the core of the evacuator

B = Flux density in the core of the evacuator

A = Cross-sectional area of core of the evacuator

The equation describes the magnetic flux developed by the magnetomotive force when a voltage applied to the circuit of the evacuator and current passes through the cross section of the magnetic core with permeability (μ). Hence, the flux density is directly proportional to permeability and magnetic field strength and is expressed as

- iii. the particles under investigation are of range size of 10 μm to 10 cm diameter and a mass of approximately 15 to 150 milligrams;
- iv. the four panels have equal dimensions, including surface area;
- v. the four panels have equal length of windings;
- vi. since the windings are connected in parallel, the electromotive force applied to each of the four panels is equal;
- vii. the permeability of the core material in each of the four panels is the same.

It therefore means that the electromagnetic fluxes in each panel will be equal. Then, the modelling of the electromagnetic flux produced by the debris evacuator in each panel of the spacecraft is described below.

3.2.3 Parameters in Panel A

The reluctance of a magnetic core is inversely proportional to the permeability and cross sectional area of the core and directly proportional to the length of the windings around it and is given as:

$$R = l/\mu\mu_r \quad (3.8)$$

where

R = Reluctance of the magnetic core of the evacuator

l = length of coil in the evacuator

μ_r = Relative permeability of the magnetic core of the evacuator

The above expression for the debris evacuator model (fig. 3.3) took into consideration the permeability of the chosen core, ferrite of nickel zinc, length of coil windings with a unit cross-sectional area and reluctance of the core.

Let equation (3.8) be expressed as

$$\Phi = \frac{F}{R} \quad (3.9)$$

The flux produced by the coil wound around magnetic core labelled 4 on panel A in the developed evacuator model (Fig. 3.3) is given as

$$\Phi_A = \frac{F_A}{R_A} \quad (3.10)$$

where,

Φ_A = flux produced in panel A

F_A = applied electromotive force in panel A

R_A = reluctance of the magnetic core 4 in panel A

Since reluctance is given as $R = l/A\mu$, then for panel A,

$$R_A = \frac{l_A}{A\mu_r} \quad (3.11)$$

where,

l_A = length of coil windings in panel A

A = cross-sectional area of the magnetic core in panel A

$\mu_r = \frac{\mu}{\mu_0}$ = relative permeability of the magnetic core and free space around panel A

Substituting equation (3.11) in (3.10) we have

$$\Phi_A = F_A \cdot \frac{A\mu_r}{l_A} \quad (3.12)$$

Similarly for panels B, C and D, the following expressions are obtainable.

For panel B

$$\Phi_B = F_B \cdot \frac{A_B}{l_B} \quad (3.13)$$

For panel C

$$\Phi_C = F_C \cdot \frac{A_C}{l_C} \quad (3.14)$$

For panel D

$$\Phi_D = F_D \cdot \frac{A_D}{l_D} \quad (3.15)$$

Since the panels are similar, then the total electromagnetic flux in the circuit of the debris evacuator is given by

$$\sum_{i=1}^4 \Phi_i = 4F_A \cdot \frac{A_A}{l_A} \quad (3.16)$$

This equation will be used to simulate the flux produced in the model developed.

The space debris evacuator is modelled to attract debris of sizes ranging from 10µm to 10cm, or mass ranging from 15 to 150mg with the aid of the integrated debris detector sensor along the graveyard orbit of LEO. The range proposed in this thesis is as a result of the range of values that can be produced from the modeled flux equation. Also, the most populous space debris falls within this range.

The reluctance, being a function of the circuit materials and the surrounding environment, can be expressed in terms of their permeability. Since soft metals have low reluctance they generate magnetic flux, forming strong temporary magnetic poles and causing a force that tends to attract other materials. The diagram shown in fig 3.5 describes the debris sizes under consideration in this thesis.

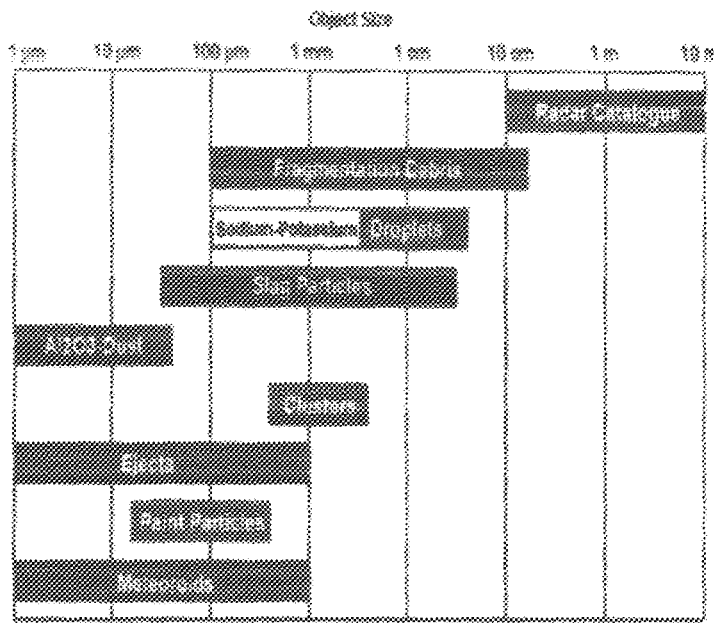


Fig. 3.5: Objects in near-earth space orbits and their respective contribution [Timothy *et al.*, 2003]

The magnetic material used in this model, is ferrite of nickel zinc wound with N number of turns, which can be varied for different magnetic flux desired. The permeability of this metal is $\mu = 20 \times 10^{-6}$ Henry per metre (H/m) and permeability in free space is $\mu_0 = 4\pi \times 10^{-7}$ Henry per metre (H/m). For illustration, consider a panel of unity cross-sectional area, the relative permeability is

$$\mu_r = \frac{\mu}{\mu_0} \quad (3.17)$$

Substituting values of μ and μ_0 respectively, $\mu_r = \frac{20 \times 10^{-6}}{4\pi \times 10^{-7}} = 16$

For a panel of the evacuator, the reluctance in the coil is $R = l/A\mu$,

Hence,

$$R = \frac{\text{length of windings}}{1 \times 16} = 1.25 \text{ Ampere-turns/Weber}$$

Similarly, this reluctance can be measured directly from the magnetic circuit using magnetic reluctance sensor, which detects change in the electromagnetic field that occurs when current passes through the coils of the ferrous metal with respect to the pole piece of the sensor probe.

In simulation, a range of values for applied magnetomotive force can be plotted against the corresponding values of electromagnetic flux produced, with different number of windings. It is noteworthy that the reluctance of the circuit may change after continuous applied voltage and may be responsible for any deviation in the expected curve. MATLAB software was used in chapter four to simulate the model and analyze the relationship between these parameters.

3.3 In-Orbit Behaviour of the Debris Evacuator

The modelled Electromagnetic Space Debris Evacuator is designated to be launched into the prescribed orbit (LEO Orbit) in a similar way to a typical spacecraft launch. The integrated system contains a range sensor that evaluates the evacuator distance to the targeted debris. The response/feedback of the range sensor sends signal to the Telemetry Control and Ranging (TC&R) in the developed model, which closes the circuits of panels A, B, C, and D and electromagnetic fluxes are generated to attract the space debris under the ranged distance, mass and size. The attractions of the nodes are subject to their mass and the magnetic flux strength developed by the evacuator. The sum of the attracted debris to the target (debris evacuator) can be simulated using an optimization technique that allows equal opportunity for all individual debris that are attracted with respect to their sizes, mass and flux impact on the debris. The strength of the evacuator holding on to the

debris is subject to the closure of the magnetic circuit and equal distribution of the magnetic flux.

The magnetic circuit, when turned on, causes the attraction of the nodes (debris) to the target (evacuator). The collections of the debris are attracted to the target making the target to have a new position, acceleration and vector characteristics. This could best be described by the perturbation force in accordance with nominal Kepler's orbital parameters. In a nominal satellite and celestial body's relationship, the sun or the moon creates a perturbing force with respect to an Earth-orbiting body that can change appreciably the parameters of its nominal Keplerian orbit. The sum of all the forces (space debris) acting on the target body (debris evacuator) is similar to the N-body equation simulation of a dynamical system of particles, usually under the influence of physical forces, such as gravity [Theraja *et al*, 1961].

3.4 Atmospheric Entry of the Debris Evacuator

The debris evacuator's re-entry into the atmosphere is achieved through ground control station; and it also depends on the initial velocity, path angle, aerodynamic drag, and evacuator mass. The process is the same for a typical manned mission re-entry. Gravitational attraction will aid the velocity of the spacecraft (evacuator) to increase as it approaches the earth. But in the absence of atmosphere, the spacecraft orbiting from its initial position at an infinite distance will accelerate to an impact velocity equal to the surface escape velocity analogous to escape velocity of object falling from space [Marcel, 1997]. During the re-entry, the evacuator switch is turned off and the released debris

would experience aerodynamic drag when the atmospheric density becomes appreciable and causes the debris to decelerate until it enters the Earth.

The free fall of the debris continues until the velocity approaches its terminal value, where atmospheric drag equals mass of the debris. At this time, the acceleration approaches zero and the evacuated debris makes a successful re-entry to the Earth at designated zones (ocean or desert) depending on the designed trajectory. Regardless of the type of entry trajectory chosen, care must be taken not to decelerate too quickly else, the evacuator will overheat and disintegrate, thus creating more debris.

CHAPTER FOUR

4.0

RESULTS

The modelling of space debris evacuator illustrated in chapter three explained component parts of the spacecraft, assumed parameters and altitude of operation. Also, the chapter explained the relationship between the evacuator and the space debris. The characteristics of the debris were assumed to have enough charges as attracting property from the solar radiation and the origin of such debris. Hence the modeled evacuator in orbit under applied forces produces fluxes that drag the debris towards itself with respect to the magnitude of the applied force and weight of the debris.

The general operation of satellites by the ground control station holds for this modelling (debris evacuator); hence, the applied voltage can be turned ON and OFF from the ground control station. The various components of the model have been used to develop a mathematical expression as shown in equation (3.16) and is simulated as shown below to produce graphs that describe relationship between the components. Matrix Laboratory (MATLAB) Software 7.4.0 was used for the simulation and the analytical procedure taken from MATLAB book published by Brain and Daniel, (2008).

The graph obtained using the mathematical equations developed in chapter three will be compared with the expected description of operation of the debris evacuator based on the assumptions made for the models. The modelled equation ($\Sigma_{i=1}^n \Phi_i = +F_s \cdot \frac{A_s}{D}$) describes the relationship between the total electromagnetic flux " Φ " and the applied magnetomotive force " F " in the panels, surface area " A " of the panel, relative

permeability " μ_r " and length of coil in the panel. The electromagnetic flux in each panel will be represented by " q ".

4.1 Analysis of the plot of magnetomotive force (F) against electromagnetic flux (q) in each panel in the Debris Evacuator

The parameters in equation (3.16) are declared for both general and assumed values in Appendix A. The MATLAB codes in appendix A are used for the simulation of the electromagnetic flux developed with respect to the applied magnetomotive force in each panel of the subsystem. After the execution of the MATLAB codes, the graph generated is shown in Fig. 4.1. In the graph, the applied magnetomotive force (F) against electromagnetic flux in each panel is represented by (q) and is plotted to give the curve of the differential equation modeled in equation (3.16). The MATLAB codes are written to calculate the value of electromagnetic flux with respect to the magnetomotive force and the plotted graph of (q) against (F) is shown in Fig. 4.1.

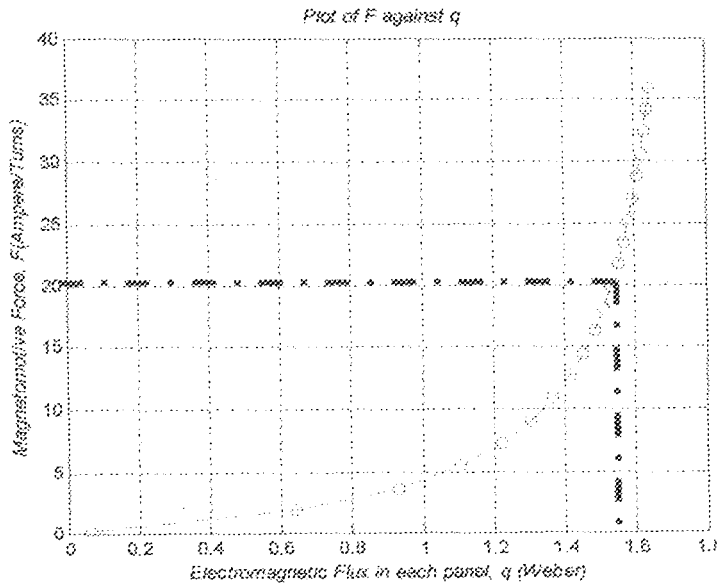


Fig. 4.1: Plot of Magnetomotive Force (F) against Panel Electromagnetic Flux (q)

Fig. 4.1 showed that the electromagnetic flux developed in each panel does not increase with corresponding increase in the magnetomotive force. As long as the panel switch is ON, the flux holds the space debris on the outside panel surface. It then means that further increase in the magnetomotive force, for instance when magnetomotive force of 21.65 Ampere/turn, is applied to the panel, the correspondence electromagnetic flux developed is 1.55 Weber. The increase continued until there is no significant increase in flux with increase in magnetomotive force as shown in the graph (fig. 4.1).

Table 4.1: MATLAB values for the simulation of magnetomotive force (F) against electromagnetic flux (q) in each panel in a unity cross-sectional area (A) and relative permeability environment (μ_r) of the debris evacuator

S/N	Length, l (m)	Magnetomotive Force, F (Ampere/turn)	Product of Magnetomotive force and area, Fa (Ampere/turn-m)	Product of Fa and μ_r (Fa) (H-A/turn)	Flux in each Panel, q (Weber)
1	2.000000	0.125000	0.125000	0.125497	0.062748
2	3.000000	1.918750	1.918750	1.926376	0.642125
3	4.000000	3.712500	3.712500	3.727256	0.931814
4	5.000000	5.506250	5.506250	5.528135	1.105627
5	6.000000	7.300000	7.300000	7.329015	1.221502
6	7.000000	9.093750	9.093750	9.129894	1.304271
7	8.000000	10.887500	10.887500	10.930773	1.366347
8	9.000000	12.681250	12.681250	12.731653	1.414628
9	10.000000	14.475000	14.475000	14.532532	1.453253
10	11.000000	16.268750	16.268750	16.333412	1.484856
11	12.000000	18.062500	18.062500	18.134291	1.511191
12	13.000000	19.856250	19.856250	19.935171	1.533475
13	14.000000	21.650000	21.650000	21.736050	1.552575
14	15.000000	23.443750	23.443750	23.536930	1.569129
15	16.000000	25.237500	25.237500	25.337809	1.583613
16	17.000000	27.031250	27.031250	27.138688	1.596393
17	18.000000	28.825000	28.825000	28.939568	1.607754
18	19.000000	30.618750	30.618750	30.740447	1.617918
19	20.000000	32.412500	32.412500	32.541327	1.627066
20	21.000000	34.206250	34.206250	34.342206	1.635343
21	22.000000	36.000000	36.000000	36.143086	1.642868

This means that fluxes have been developed in the panel with the maximum magnetomotive force applied which is required for the attraction of the space debris within the sensor region of the evacuator. The analysis showed that the development of the required flux can be driven by the initial applied voltage of 10Volts to the Electromagnetic Control Subsystem (EMS) shown in Fig. 3.1. Also, the analysis of the generated and tabulated values from the MALAB simulation is shown in table 4.1. The relationship between the magnetomotive force and the electromagnetic flux in each panel can be easily deduced using Table 4.1.

4.2 Analysis of the plot of Length of coil (l) against Magnetomotive Force (F) in each panel of the Debris Evacuator

The MATLAB codes in Appendix B are used for the simulation of the length of coil the in each panel with respect to magnetomotive force in each panel of the subsystem. The MATLAB codes are written to calculate and plot the graph of magnetomotive force (F) against length (l) of coil in evacuator. After the execution of the MATLAB codes, the graph generated is shown in Fig. 4.2.

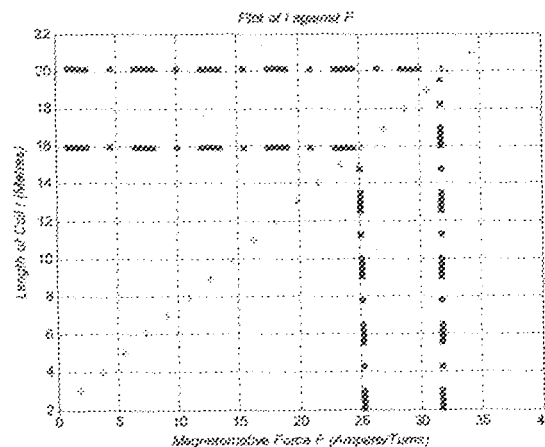


Fig. 4.2: Plot of Length of coil against Magnetomotive Force

As seen in the graph, the magnetomotive force developed in each panel is proportional to the length of coil in the panel. From the graph; when the length of the coil is 16 m, the corresponding magnetomotive force is 25.24 Ampere/turn and also when the length of the coil is 20 m, the corresponding point on the axis of magnetomotive force will be 32.41 Ampere/turn. Either of the values of the length of the coil and the magnetomotive force can be calculated using Fig. 4.2. The variation of the length of the coil and the magnetomotive force would be required to produce different fluxes needed for the evacuation of the space debris under examination.

Table 4.2: MATLAB values for the simulation of length of coil (l) against Magnetomotive Force (F) in each panel in a unity cross-sectional area (A) and relative permeability environment (μ_r) of the debris evacuator.

S/N	Length l (m)	Magnetomotive Force, F (Ampere/turn)	Product of Magnetomotive force and area, Fa (Ampere/turn-m)	Product of Fa and μ_r (Fa)(H-A/turn)	Flux in each Panel, ϕ (Weber)
1	2.000000	0.125000	0.125000	0.125497	0.062748
2	3.000000	1.918750	1.918750	1.926376	0.642125
3	4.000000	3.712500	3.712500	3.727256	0.931814
4	5.000000	5.506250	5.506250	5.528135	1.105627
5	6.000000	7.300000	7.300000	7.329015	1.221502
6	7.000000	9.093750	9.093750	9.129894	1.304271
7	8.000000	10.887500	10.887500	10.930773	1.366347
8	9.000000	12.681250	12.681250	12.731653	1.414628
9	10.000000	14.475000	14.475000	14.532532	1.453253
10	11.000000	16.268750	16.268750	16.333412	1.484856
11	12.000000	18.062500	18.062500	18.134291	1.511191
12	13.000000	19.856250	19.856250	19.935171	1.533475
13	14.000000	21.650000	21.650000	21.736050	1.552575
14	15.000000	23.443750	23.443750	23.536930	1.569129
15	16.000000	25.237500	25.237500	25.337809	1.583613
16	17.000000	27.031250	27.031250	27.138688	1.596393
17	18.000000	28.825000	28.825000	28.939568	1.607754
18	19.000000	30.618750	30.618750	30.740447	1.617918
19	20.000000	32.412500	32.412500	32.541327	1.627066
20	21.000000	34.206250	34.206250	34.342206	1.635343
21	22.000000	36.000000	36.000000	36.143086	1.642868

Table 4.2 shows the interrelationship between the length of the coil and the magnetomotive force produced by each panel. From the table; at any particular value of the length of the coil, a corresponding value of magnetomotive force can be obtained and vice-versa, then the ratio of electromagnetic flux and the length of the coil can be determined. This analysis showed that the magnitude of the magnetomotive force in the panel can be increased with discrete increase in the length of coil as shown in modelled equation (3.16). The analysis of the generated and tabulated values from the MATLAB simulation is shown in table 4.2.

Since electromagnetic flux is directly proportional to the ratio of magnetomotive force and length of the coil, then the constant of proportionality, relative permeability of a unit cross-sectional area, can be easily determined with the help of the table.

4.3 Analysis of the plot of magnetomotive force (F) against Total electromagnetic flux (Q_{total}) for the Debris Evacuator

The parameters in equation (3.16) are declared for both general and assumed values in Appendix C. The MATLAB codes in Appendix C are used for the simulation of the total electromagnetic flux developed in the four panels with respect to the applied magnetomotive force of the subsystem. After the execution of the MATLAB codes, the graph generated is shown in Fig. 4.3. In the graph, total electromagnetic flux in each panel (Q_{total}) gives the curve of the differential equation modeled in equation (3.16). The MATLAB codes are written to calculate the value of total electromagnetic flux. The plotted graph of (F) against (Q_{total}) is shown in Fig. 4.3.

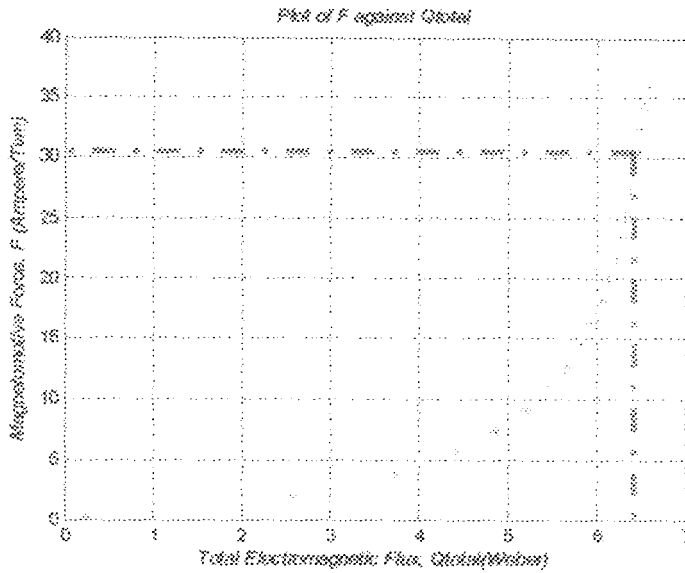


Fig. 4.3: Plot of Magnetomotive Force (F) against Total Electromagnetic Flux (Q_{total})

The graph showed that the total electromagnetic flux developed increases exponentially with increase in magnetomotive force from about 5 Ampere/Turn to about 30.61 Ampere/Turn in the subsystem and corresponding increase in electromagnetic flux goes until it reaches a above 6.47 Weber when it becomes constant with further increase in the magnetomotive force. This indicates that as long as the subsystem switch is ON, the developed flux holds the space debris on all the outside panels' surface. It then means that further increase in the magnitude of the flux will depend on other parameters, such as length of coil and surface area of the panel. Also, the analysis of the generated and tabulated values from the MALAB simulation is shown in table 4.3.

As shown in Table 4.3, the value of Q_{total} is four times the value of q in Table 4.2 as illustrated in equation (3.16).

Table 4.3: MATLAB values for the simulation of Total electromagnetic Flux (Q_{total}) against magnetomotive force (F) of the debris evacuator in a unity cross-sectional area (A) and relative permeability environment (μ_r) of the debris evacuator.

S/N	Length, l (m)	Magnetomotive Force, F (Ampere/turn)	Product of Magnetomotive force and area, Fa (Ampere/turn- m)	Product of Fa and μ_r , (Fa) (H-A/turn)	Flux in each Panel, ϕ (Weber)	Q_{total} in the evacuator (Weber)
1	2.000000	0.125000	0.125000	0.125497	0.062748	0.250994
2	3.000000	1.918750	1.918750	1.926376	0.642125	2.568502
3	4.000000	3.712500	3.712500	3.727256	0.991814	3.727256
4	5.000000	5.506250	5.506250	5.528135	1.105627	4.422508
5	6.000000	7.300000	7.300000	7.329015	1.221502	4.886010
6	7.000000	9.093750	9.093750	9.129894	1.304271	5.217082
7	8.000000	10.887500	10.887500	10.930773	1.366947	5.465387
8	9.000000	12.681250	12.681250	12.731653	1.414628	5.658512
9	10.000000	14.475000	14.475000	14.532532	1.453253	5.813013
10	11.000000	16.268750	16.268750	16.333412	1.484856	5.939422
11	12.000000	18.062500	18.062500	18.134291	1.511191	6.044764
12	13.000000	19.856250	19.856250	19.935171	1.533475	6.133899
13	14.000000	21.650000	21.650000	21.736050	1.552575	6.210300
14	15.000000	23.443750	23.443750	23.536930	1.569120	6.276515
15	16.000000	25.237500	25.237500	25.337809	1.583613	6.334452
16	17.000000	27.031250	27.031250	27.138688	1.596393	6.385574
17	18.000000	28.825000	28.825000	28.939568	1.607754	6.431015
18	19.000000	30.618750	30.618750	30.740447	1.617918	6.471673
19	20.000000	32.412500	32.412500	32.541327	1.627066	6.508265
20	21.000000	34.206250	34.206250	34.342206	1.635349	6.541373
21	22.000000	36.000000	36.000000	36.143086	1.642868	6.571470

CHAPTER FIVE

5.0 DISCUSSION, CONCLUSIONS AND RECOMMENDATIONS

5.1 Discussion

The modelled space debris evacuator in the low Earth orbits is an improvement on the previous efforts which were only descriptive techniques for debris mitigation. The configuration of the space debris evacuator (fig. 3.2) showed the subsystems and the integration of the evacuator which was modelled as a typical spacecraft. The launch and operation are achieved with the use of a ground station control which allows the evacuator to be turned ON to attract space debris when in the preferred orbit and is turned OFF after maneuvering it to the orbit of discharge (near earth orbit). The modelled equation (3.16) was simulated using MATLAB analysis software with respect to the parameters in the equation. The resulting graph in fig 4.2 showed that the magnetomotive force in the evacuator can be increased linearly with increase in the length of the coils which, in turn produces the electromagnetic flux required to attract the space debris. The station keeping of the evacuator is achieved with the ground station control.

Fig. 4.1 and fig. 4.3 showed the graphs of the simulation of the modelled equation for the electromagnetic flux of the debris evacuation from the operational orbits. At any particular value of the length of the coil, a corresponding value of magnetomotive force can be obtained and vice-versa; then, the ratio of electromagnetic flux and the length of the coil can be determined. Since electromagnetic flux is directly proportional to the ratio of magnetomotive force and length of the coil, then the constant of proportionality, relative permeability of a unit cross-sectional area, can be easily determined.

5.2 Conclusions

The space debris mitigation must be addressed collectively by all space fairing nations both at mission planning and end of mission for better space environment and lesser risk on Earth environment.

The implementation of a space debris evacuator cannot be by individual organization or a nation's responsibility but by collective efforts of nations because of its high risk and cost, especially the operation in orbit involving different missions and frequency coordination. Until a re-entry and re-use of the evacuator are ascertained, the cost of single mission for an evacuator may be high. Other debris mitigation techniques such as space shuttle or drag net also prove that debris evacuators are expensive. Because of the complexity of operation and cost, the work on the re-entry is recommended for a doctoral degree.

In the operation of a space debris evacuator, it may not be certain if satellite in the orbits near its operation will be safe from residual drag and the corresponding implication on autonomous and ground controlled missions. Hence, the International Telecommunication Union (ITU) must intervene in the proof of concept (model) if space fairing nations must be involved in this technique of debris mitigation.

5.3 Recommendations

The study has identified the measures to reduce the number of space debris or reduce the hazards created by space debris and should be accepted for criticism, which includes:

- Identification of space debris sources
- Design and operation of space systems to avoid or reduce the creation of space debris
- Removal of man-made objects
- Measures to prevent the creation of space debris
- Measures to reduce the collision hazard and guidelines for debris mitigation.

REFERENCES

- Bariteau M. and Mandeville J. (2002), "*Modelling of ejecta as a space debris*", 2nd Edition, NASA, Houston, USA, pp. 97-107.
- Brain H. and Daniel T. V, (2008), *Essential Matrix Laboratory (MATLAB) for Engineers and Scientists*, Third Edition, Elsevier, United Kingdom, pp. 170-175.
- Breukelen E, Bergsma O, Maessen D and Zandbergen B, (2006), "*Development of a Generic Inflatable De-Orbit Device*", Delft University of Technology,
- Christiansen E and Lear D. (1996), "*Handbook for space shuttle meteoroid/orbital debris threat assessments*", Aerospace Engineering, Vol, 221, USA, pp 975-980.
- IADC, (2003) "*Space Debris Mitigation Guidelines*" Space debris A/AC.105/C.1/L.260, UN COPUOS 40th session, Austria, pp 2-9.
- Jonathan W. C. (2000), "*Laser Orbital Debris Removal and Asteroid Deflection*", Center for Strategy and Technology, Alabama, USA, pp 6-12.
- Johnson, N. L., Whitlock, D. O., and Anz-Meador, P. D. (2004), "*History of on-orbit satellite fragmentations*", 13th edition, NASA, USA, pp 9-15.
- Marcel J. S. (1997), *Spacecraft Dynamics and Control: A Practical Engineering Approach*, Press Syndicate of the University of Cambridge, USA, pp. 1-113.
- Megan H. (2009) "*Duo of Canadian Sats in Debris Danger*," Satnews Daily, USA, pp 15.
- Stansbery, G. and Foster, J. L. (2005), "*Completeness of measurements of the orbital debris environment*", 4th European Conference on Space Debris, ESA, France, pp. 95-100.
- Theraja B. L. and Theraja A. K. (1961), *A Text-Book of Electrical Technology*, Nirja Construction, New Delhi, pp 162-189.

Appendices

MATLAB Simulation of Flux Produced in the Debris Evacuator

Appendix A

Script 1

To calculate and plot magnetomotive force (F) against electromagnetic flux (q) in each panel

```
% Script file: Plot of magnetomotive force (F) against electromagnetic flux (q) in each
panel
%
% Purpose:
% To calculate the value of q and F, and to plot F against q
%
% Record of revisions:
%   Date      Programmer   Description of change
%   =====
%   02/03/10  Odimayomi P.K.      Original Code
%
% Define variables
% F    --   Magnetomotive force
% Fa   --   Product of magnetomotive force and area
% Fx   --   Product of Fa and Ur
% A    --   Area of the panel
% U    --   Permeability of ferrite of nickel zinc
% Ur   --   Relative permeability
% Uo   --   Permeability of free space
% l    --   length of the coil
% q    --   Electromagnetic flux

% Clear screen
clc

U = 20.10^-6;
Uo = 13.10^-7;
A = 1;

% Create an array of length
l = 2:1:22;

% Calculate Relative permeability
Ur = U/Uo;

% Create an array of the magnetomotive force F
```

```

F = 0.125:1.79375:36;

% Calculate relative permeability
Ur = U/Uo;

% Calculate the value of flux and area
Fa = F*A;

% Product of Fa and Ur
Fx = Fa*Ur;

% Calculate the value of electromagnetic flux
q = Fx./A;

% Plot the graph of F against q

plot(q, l, 'bo--');
xlabel('\itElectromagnetic flux in each panel, q');
ylabel('\itMagnetomotive force , F');
title('\itPlot of F against q ');
grid on;

% Display results
fprintf('l = %8.6fn', l);
fprintf('A = %8.6fn', A);
fprintf('F = %8.6fn', F);
fprintf('q = %8.6fn', q);
fprintf('Fa = %8.6fn', Fa);
fprintf('Fx = %8.6fn', Fx);

```

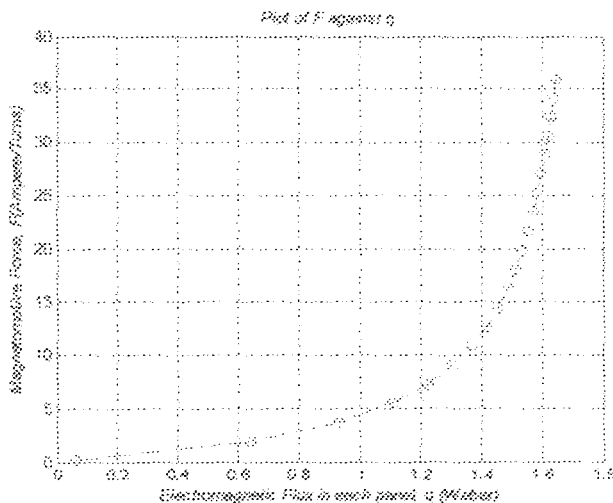


Fig. 4.1: Plot of Magnetomotive Force (F) against Panel Electromagnetic Flux (q)

Appendix B

Script 2

To calculate the Length of coil (l) against Magnetomotive Force (F), and to plot (F) in the Debris Evacuator

```
% Script file: Flux produced by Debris Evacuator
%
% Purpose:
% To calculate the value of Magnetomotive Force F, and to plot Length of coil l against
Magnetomotive Force F
%
% Record of revisions:
%   Date   Programmer   Description of change
%   =====
%   02/03/10 Odimayomi P.K.   Original Code
%
% Define variables
% F    -- Magnetomotive force
% Fa   -- Product of magnetomotive force and area
% Fx   -- Product of Fa and Ur
% A    -- Area of the panel
% U    -- Permeability of ferrite of nickel zinc
% Ur   -- Relative permeability
% Uo   -- Permeability of free space
% l    -- length of the coil
% q    -- Electromagnetic flux
% Qtotal -- Total electromagnetic flux

% Clear screen
clc

U = 20.10^-6;
Uo = 13.10^-7;
A = 1;

% Create an array of length
l = 2:1:22;

% Calculate Relative permeability
Ur = U/Uo;

% Create an array of the magnetomotive force F
F = 0.125:1.79375:36;
```

```

% Calculate relative permeability
Ur = U/Uo;

% Calculate the value of flux and area
Fa = F*A;

% Product of Fa and Ur
Fx = Fa*Ur;

% Calculate the value of electromagnetic flux
q = Fx./l;

% Create the plot of L against F

plot(F, l, 'g*-');
title('\itPlot of F against l');
xlabel ('\itMagnetomotive force, F');
ylabel ('\itLength of the coil, l');
legend ('\it l versus F');
grid on;

% Display results
fprintf('l = %8.6fn', l);
fprintf('A = %8.6fn', A);
fprintf('F = %8.6fn', F);
fprintf('q = %8.6fn', q);
fprintf('Qttotal = %8.6fn', Qttotal);
fprintf('Fa = %8.6fn', Fa);
fprintf('Fx = %8.6fn', Fx);

```

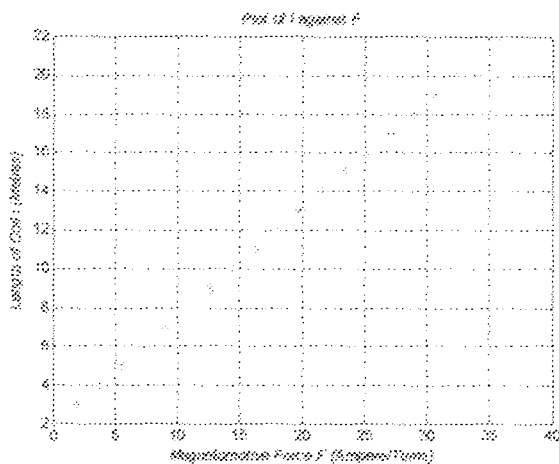


Fig. 4.2: Plot of Length of coil against Magnetomotive Force

Appendix C

Script 3

Plot of magnetomotive force (F) against Total electromagnetic flux (Q_{total}) for the Debris Evacuator

```
% Script file: Plot of magnetomotive force (F) against Total electromagnetic flux (Qtotal) for the Debris Evacuator
```

```
%
```

```
% Purpose:
```

```
% To plot the graph of F against Qtotal
```

```
%
```

```
% Record of revisions:
```

```
%      Date      Programmer      Description of change
```

```
% =====
```

```
% 02/03/10      Odimayomi P.K.      Original Code
```

```
%
```

```
% Define variables
```

```
% F -- Magnetomotive force
```

```
% Fa -- Product of magnetomotive force and area
```

```
% Fx -- Product of Fa and Ur
```

```
% A -- Area of the panel
```

```
% U -- Permeability of ferrite of nickel zinc
```

```
% Ur -- Relative permeability
```

```
% Uo -- Permeability of free space
```

```
% l -- length of the coil
```

```
% q -- Electromagnetic flux
```

```
% Qtotal -- Total electromagnetic flux
```

```
% Clear screen
```

```
clc
```

```
U = 20.10^-6;
```

```
Uo = 13.10^-7;
```

```
A = 1;
```

```
% Create an array of length
```

```
l = 2:1:22;
```

```
% Calculate Relative permeability
```

```
Ur = U/Uo;
```

```
% Create an array of the magnetomotive force F
```

```
F = 0.125:1.79375:36;
```

```
% Calculate relative permeability
```

```
Ur = U/Uo;
```

```

% Calculate the value of flux and area
Fa = F*A;

% Product of Fa and Ur
Fx = Fa*Ur;

% Calculate the value of electromagnetic flux
q = Fx./l;

% Calculate the electromagnetic flux produced by the panels
Qtotal = 4*(Fx./l);

% Plot the graph of magnetomotive force (F) against total electromagnetic flux (Qtotal)
%

plot(Qtotal, F, 'm*--');
xlabel('\itTotal Electromagnetic Flux, Qtotal');
ylabel('\itMagnetomotive Force, F');
title('\itPlot of Qtotal against F');
grid on;

% Display results
fprintf('l = %8.6fn', l);
fprintf('A = %8.6fn', A);
fprintf('F = %8.6fn', F);
fprintf('q = %8.6fn', q);
fprintf('Qtotal = %8.6fn', Qtotal);
fprintf('Fa = %8.6fn', Fa);
fprintf('Fx = %8.6fn', Fx);

```

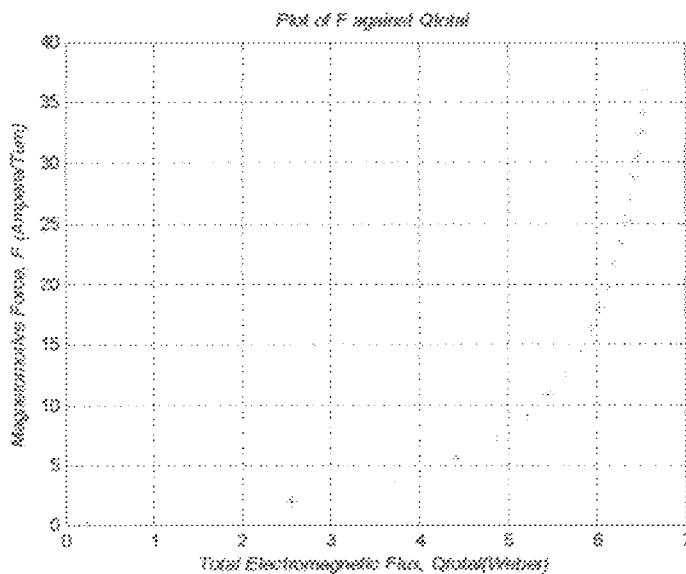


Fig. 4.3: Plot of Magnetomotive Force (F) against Total Electromagnetic Flux (Q_{Total})